NBER WORKING PAPER SERIES

# GLOBAL NATURAL RATES IN THE LONG RUN: POSTWAR MACRO TRENDS AND THE MARKET-IMPLIED R* IN 10 ADVANCED ECONOMIES

Josh Davis
Cristian Fuenzalida
Leon Huetsch
Benjamin Mills
Alan M. Taylor

Working Paper 31787
http://www.nber.org/papers/w31787

NATIONAL BUREAU OF ECONOMIC RESEARCH
1050 Massachusetts Avenue
Cambridge, MA 02138
October 2023

For helpful comments and discussions we thank Ben Bernanke, Joachim Fels, participants in seminars at the Federal Reserve Bank of San Francisco and Stanford University, and the NBER ISOM conference organizers, board, participants, and our discussants ukasz Rachel and David Thesmar. All errors are ours. Disclaimer: The views and opinions expressed in this paper are those of the author(s) and do not necessarily reflect the official policy or position of Graham Capital Management. The research presented herein is the work of the author(s) and should not be attributed to Graham Capital Management or its affiliates. The views expressed herein are those of the authors and do not necessarily reflect the views of the National Bureau of Economic Research.

At least one co-author has disclosed additional relationships of potential relevance for this research. Further information is available online at http://www.nber.org/papers/w31787

Global Natural Rates in the Long Run: Postwar Macro Trends and the Market-Implied r* in 10 Advanced Economies

Josh Davis, Cristian Fuenzalida, Leon Huetsch, Benjamin Mills, and Alan M. Taylor

NBER Working Paper No. 31787
October 2023
JEL No. C13,C32,E43,E44,E47,G12

## ABSTRACT

Benchmark finance and macroeconomic models appear to deliver conflicting estimates of the natural rate and bond risk premia. This natural rate puzzle applies not only in the U.S. but across many advanced economies. We use a unified no-arbitrage macro- finance model with two trend factors to estimate the natural rate r* for 10 advanced economies. We cover a longer and wider sample than previous studies and draw on new sources to construct yield curves and excess returns. The two-trend model improves the explanatory power of yield regressions and return forecasts. Most variation in yields is due to the macro trends r* and *, and not bond risk premia. Global components of unexpected bond returns are influential, while the local components of natural rates are large. Our r* estimates covary with growth and demographic variables in a manner consistent with theory and previous findings.

Josh Davis
PIMCO
650 Newport Center Drive
Newport Beach CA 92660
josh.davis@pimco.com

Benjamin Mills
PIMCO
650 Newport Center Drive
Newport Beach, CA 92660
ben.mills@pimco.com

Cristian Fuenzalida
Graham Capital Management
cristian.fuenzalida@nyu.edu

Alan M. Taylor
Department of Economics and
Graduate School of Management
University of California
One Shields Ave
Davis, CA 95616-8578
and CEPR
and also NBER
amtaylor@ucdavis.edu

Leon Huetsch
University of Pennsylvania
lhuetsch@sas.upenn.edu

# 1. Introduction

Studies of the natural rate and bond risk premia in the macro and finance literatures take different tracks. The objects of interest is clear and important: bond pricing and rates of interest, at all maturities, matter for saving, investment, capital allocation, economic growth, monetary policy, and so on. The macro track emphasizes low-frequency trends in Wicksellian models: the natural rate links to the rate of growth with no financial market information (e.g, Holston, Laubach, and Williams, 2017; Rachel and Summers, 2019; Jordà and Taylor, 2019); The finance track emphasizes cross-sectional no-arbitrage models of yields with higher-frequency factors and no macro information (e.g, Litterman and Scheinkman, 1991; Piazzesi, 2010; Adrian, Crump, and Moench, 2013).

Perhaps unsurprisingly, such different approaches can lead to very different estimates of natural rates and risk premia and the associated historical interpretations and narratives. We call this the *natural rate puzzle*. and we present a new empirical approach which jointly disciplines estimates of the natural rate and risk premia with both financial market *and* macro information to obtain a *market-implied natural rate* $r^*$. We first document the puzzle, for both the U.S. and other countries. For clarity, we do nothing new here: we use only on off-the-shelf models and data. The analysis revolves around three trend estimates. For the U.S., we use an estimate of the bond risk premium following the canonical model (Adrian, Crump, and Moench, 2013) used by policymakers, academics, and financial professionals. We estimate inflation expectations following research incorporating trend inflation into models of bond yields and risk premia (Cieslak and Povala, 2015). And we employ or construct an estimate of the natural rate using the seminal model in the macro literature (Laubach and Williams, 2003). We then use a decomposition of long-dated forwards based on theory to show a contradiction between estimates and natural rates and bond risk premia. The puzzle is not an artifact of these particular estimates, and obtains using other well-respected estimates of U.S. bond risk premia, trend inflation, and the natural rate from multiple credible sources. The same puzzle also exists internationally in data we have constructed similarly for 9 other advanced economies.

To tackle this conflict we set out a unified macro-finance model to ground the empirical work that follows. Here, what *we* will mean by "macro-finance" is a model that incorporates simultaneously higher-frequency insights from the yield curve in finance models and lower-frequency secular inflation and growth trends (as distinct from cyclical macro phenomena within the business cycle). The model crystallizes the uncontroversial view—among macroeconomists, at least—that nominal bond returns must include compensation for macroeconomic risks linked to real factors and inflation (Ang and Piazzesi, 2003; Ludvigson and Ng, 2009; Cieslak and Povala, 2015). It is long understood that term structure models should allow all nominal rates to include a slow-moving stochastic trend, as in Campbell and Shiller (1987). The idea was taken further in the seminal papers of Kozicki and Tinsley (2001) and Cieslak and Povala (2015), in models of shifting endpoints with a short-rate process linked to two macroeconomic factors, $r^*$ and $\pi^*$, the natural rate and inflation trends; another recent example is Bauer and Rudebusch (2020), with a single stochastic trend, a nominal natural rate factor $i^*$; all of these papers focus on U.S. evidence.

In the empirical core of the paper, we take the model to the 10-country postwar data, a global historical laboratory considerably larger than any previously explored, deriving new estimates of the natural rate covering more countries and more decades. We find strong support for the model. Trend inflation is treated as an observable and the unobservable natural rate is treated as latent and estimated from a no-arbitrage state-space model, with both macro and finance blocks, using the Kalman filter. The macro side uses a canonical Wicksellian $r^* = g + z$ state equation, and the finance side uses a canonical yield measurement equation, so our model uses information from both domains. Dropping either trend significantly worsens the model fit, especially in return forecast regressions. Indeed, as is well known, the macroeconomic factors subsume much of the relevant information needed to predict returns as compared with yield-only term-structure models, leaving only detrended yields to play a role, amplifying the insights of Cieslak and Povala (2015), and echoing Bauer and Rudebusch (2020), but now for two trends and more countries.

To sum up: First, we document an important macro-finance puzzle which the separate strands of risk premia research and natural rate research have skirted around. Second, to operationalize the model, we apply a joint macro-finance estimation strategy; though novel, and computationally more burdensome, this might be preferred to approaches which draw from disparate models. Third, we put together a new database of zero-coupon yield curves for ten countries, a valuable data contribution in its own right for the use of future researchers. Fourth, using these data and other proxies, we present estimates from a long and wide sample of 10 advanced economies and identify various global trends. Fifth, our method produces improved predictions for bond yields and returns in the U.S. and international samples, including out of sample return prediction. Sixth, our natural rate estimates covary with growth and demographic variables in a manner consistent with theory and previous findings. Lastly, most of the long-term variation in yields in recent decades has come from shifts in the natural rate and inflation trend components, not from shifts in bond risk premia.

## 2. The natural rate puzzle

In the class of standard no-arbitrage bond-pricing models, the term structures (of bond yields and prices, excess returns, and forwards) are affine functions of a vector of risk factors $F$. This will be made precise in the next section, where we demonstrate that, in such models where Fisher constraints hold, we can express the long-maturity forward rate, in the limit, as

$$\text{limiting forward rate} \;=\; \text{natural rate trend} \;+\; \text{inflation trend} \;+\; \text{limiting risk premium}\,. \qquad (1)$$

This shorthand expression is transparent and intuitive—so much so that in the bond market many practitioners view the state of pricing and risk premia at the long end through exactly this lens. Investors in long-maturity forwards must be compensated by the sum of the natural rate and inflation trend values, plus a long-maturity bond risk premium. Derived below as a theoretical limit the formula sheds light on how we can decompose rates into macro trends and risk premia.

It is immediately tempting to try to validate the empirical content of Equation 1 by taking extant proxies for each term and checking to see if they add up approximately. We now attempt this, but as flagged above, we will end up disappointed, finding that the margins of error are uncomfortably large. Specifically, we naïvely take a long-maturity risk premium (denoted $RP$) from benchmark models in the finance literature, we take the latent natural rate trend estimate (denoted $r^*$) from benchmark macro models, we take the observable inflation trend (denoted $\pi^*$) from various proxies or survey measures, and we take a proxy long-maturity forward rate (denoted $f$) derived from observable market data using an estimate of the zero-coupon curve, as described below. Having constructed these four terms for multiple countries, we show that the above equation fails to hold.

This is what we term the *natural rate puzzle*. This section documents this fact across the advanced economies. The rest of the paper then explores a hybrid macro-finance model by which the puzzle could be ameliorated. As might be anticipated, Equation 1 offers only two escape routes. Assuming that the forward rate is known, and the inflation trend $\pi^*$ is not subject to large estimation error, and can also be treated as quasi-observable, then either the unobservable trend in the natural rate $r^*$ is mismeasured, or the unobservable trend in the risk premium $RP$ is mismeasured, or both.

## 2.1. U.S. evidence

To see the puzzle we take Equation 1 to the data. In Figure 1, Panel (a), the U.S. time-series estimates for each of the four terms are shown. We simply take these estimates from canonical models in the finance and macro literatures. The bond risk premium term $RP$ (two-sided) is from the baseline five-factor model of Adrian, Crump, and Moench (2013) [henceforth abbreviated ACM]; the inflation expectations term $\pi^*$ is the Cieslak and Povala (2015) measure $\pi^*_t = (1-\nu)\sum_{i=0}^{t-1} \nu^i \pi_{t-i}$, where $\pi_t$ is year-on-year CPI inflation in month $t$. and the (two-sided) natural rate term $r^*$ as in Laubach and Williams (2003) [LW]. Finally, we proxy $f$ with the long-dated 10-year, 10-year forward rate taken from Bloomberg, with $n = m = 120$ months here.

The first version of the consistency test rearranges Equation 1 to obtain a formula for the real natural rate $r^*_{(implied)} = f - \pi^* - RP$, and Panel (b) plots both sides of this expression using the above data sources: the left-hand side is taken from an LW model and the right-hand side is the implied value using an ACM model. The equality is violated, and the disparity is often quite large. The ACM-implied $r^*$ does not match the LW $r^*$. The ACM series starts around +2% in the 1960, displays a sharp decline to a level below –2% during the Great Inflation period of the 1970s, returns to +2% in the 1990s, drops to near zero after the financial crisis, and then shows a consistent increase after 2013 to a level close to 2% in 2019. In contrast, the familiar LW estimate of $r^*$ has fallen gradually from a +4% level in the 1960s and 1970s, with the sharpest decline occurring after the mid-2000s, and since 2010 it has sat in the 0.5%–1.0% range, and never turned negative. The difference between the two series, before the last decade, is often large, between 100 and 600 basis points (bps), with the LW $r^*$ much higher than the ACM $r^*$, on average. Around 2012 the two series intersected and then the difference inverted to about –100 bps in the other direction.

**Figure 1:** *The natural rate puzzle in U.S. data*

The figure is based on Equation 1, which we can rewrite in simplified form as $f = r^* + \pi^* + RP$. In Panel (a), the four terms are shown: the bond risk premium $\Gamma$ from Adrian, Crump, and Moench (2013); inflation expectations $\pi^*$ from Cieslak and Povala (2015); and the real natural rate $r^*$ from Laubach and Williams (2003). We also show the 10-year, 10-year forward rate ($f$) from from Bloomberg. The sample period is June 1961–July 2022. In Panel (b), we compare the real natural rate $r^*$ (two-sided) from Laubach and Williams (2003) to that implied by $r^*_{(implied)} = f - \pi^* - RP$. In Panel (c), we compare the bond risk premium $RP$ (two-sided) from Adrian, Crump, and Moench (2013) to that implied by $RP_{(implied)} = f - r^* - \pi^*$.

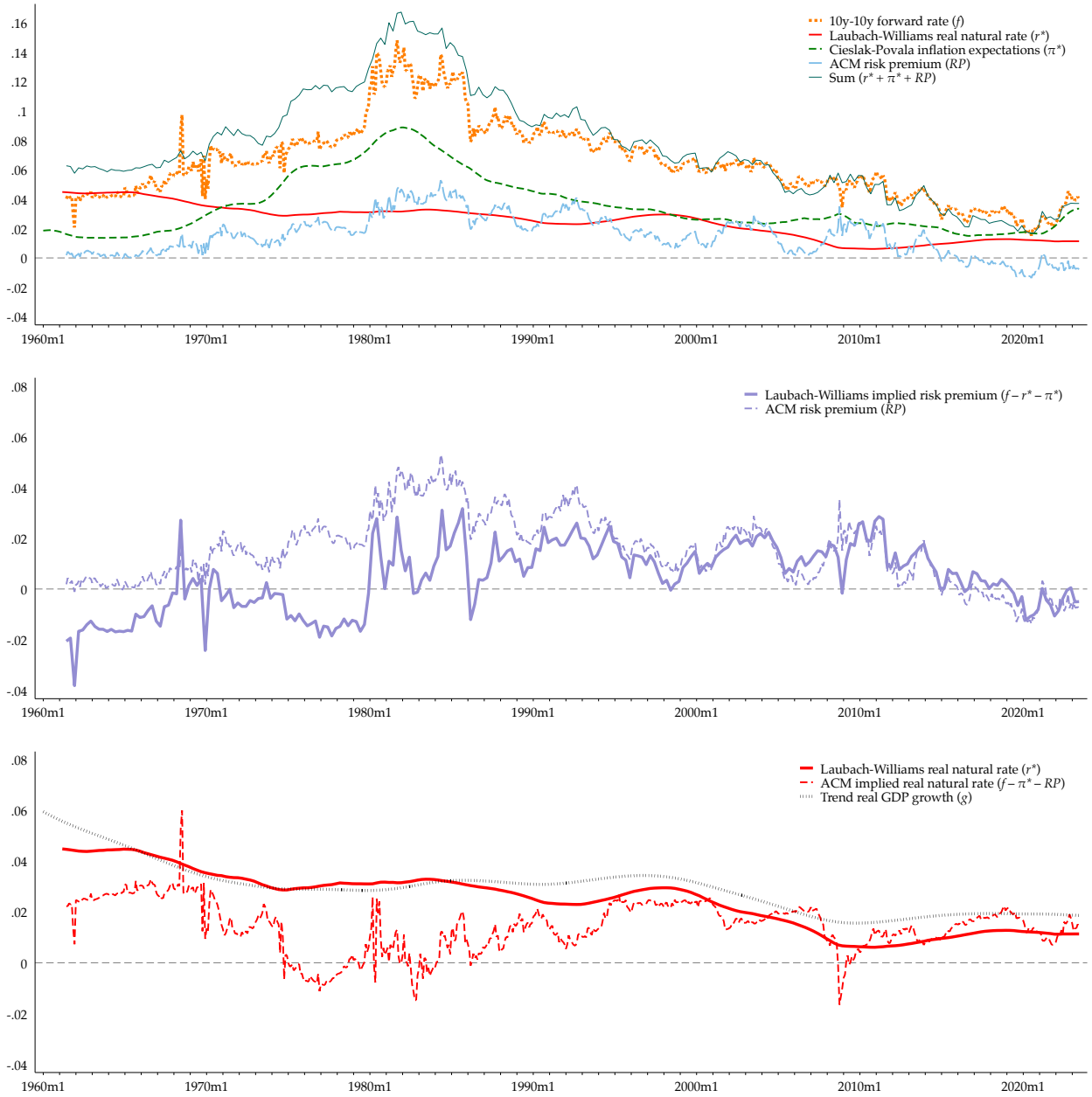

A second, equivalent, version of the test is shown in Panel (c). We rearrange again to obtain a formula for the bond risk premium $RP_{(implied)} = f - r^* - \pi^*$, and plot both sides of this expression using the aforementioned data sources. Now the left-hand side is from an ACM model and the right-hand side is the implied value in an LW model. This equality is, of course, also violated, and the same large disparity is seen. The ACM bond risk premium starts near zero in the 1960s, rises sharply in the Great Inflation period of the 1970s to about 6%, then gradually falls back, reaching zero again in the mid-2010s. The LW bond risk premium behaves very differently, and is almost flat by comparison. It actually starts at a negative level in the 1960s, rises much later, but only to a modest 2% by the early 1980s, then declines by a small amount up to the mid 2000s. After that the two series cross, with LW signaling a small positive bond risk premium, but ACM turning negative.

## 2.2. Alternative trend measures

As a robustness check, Figure 2 examines whether the existence of the puzzle for the U.S. is sensitive to the source data used for each of the elements in the calculation. For a variety of widely used and respected sources for each element we compute the discrepancy in Equation 1 as $discrepancy = RP - RP_{(implied)} = RP - (f - r^* - \pi^*)$, and plot the series over time.

The same forward rate data $f$ from Bloomberg are used in all cases. The sources of the other three series rotate through all possible combinations, with the sources are abbreviated as follows:

- Natural rate estimates $r^*$: Laubach and Williams (2003) [LW]; Del Negro, Giannone, Giannoni, and Tambalotti (2017) [DGGT]; and Lubik and Matthes (2015) [LM].
- Inflation estimates $\pi^*$: Cieslak and Povala (2015) [CiP]; the the Survey of Professional Forecasters [SPF]; the Federal Reserve Bank of Philadelphia surveys [PHIL]; University of Michigan Inflation Expectations from FRED [MI]; and the TIPS 10-Year Breakeven Inflation Rate from FRED [TIPS].
- Bond risk premium estimates $\Gamma$: Adrian, Crump, and Moench (2013), 5-factor model [ACM5]; and Kim and Wright (2005), 3-factor model [KW].

Note that because quite a few of these series (e.g., TIPS, KW) are only available for a shorter span of recent years, full-sample comparisons across all trend estimates are not always possible.

The figure reveals that the natural rate puzzle is a quite robust phenomenon in recent U.S. data. A discrepancy arises in all cases. It is often more than 100 bps, and at certain times it exceeds 500 bps. It is present in a wide variety of trend estimates currently used in the macro-finance literatures. The figure shows that, as in the baseline variant above, the extent of the puzzle varies from year to year, and over decades. Most series combinations make errors in one direction, but a few go the other way. The discrepancies are large in the 1970s, and often surge to their highest levels around 1980. The discrepancies are smaller by the late 1990s and early 2000s, but they open up again for some series, in the opposite direction to the vicinity of –200 bps, after the global financial crisis.

**Figure 2:** *The natural rate puzzle in U.S. data using alternative trend measures*

This chart displays the discrepancy in Equation 1 for the United States. The presentation is based on Equation 1 and the series computed is *discrepancy* = $RP - (f - r^* - \pi^*)$. See text.

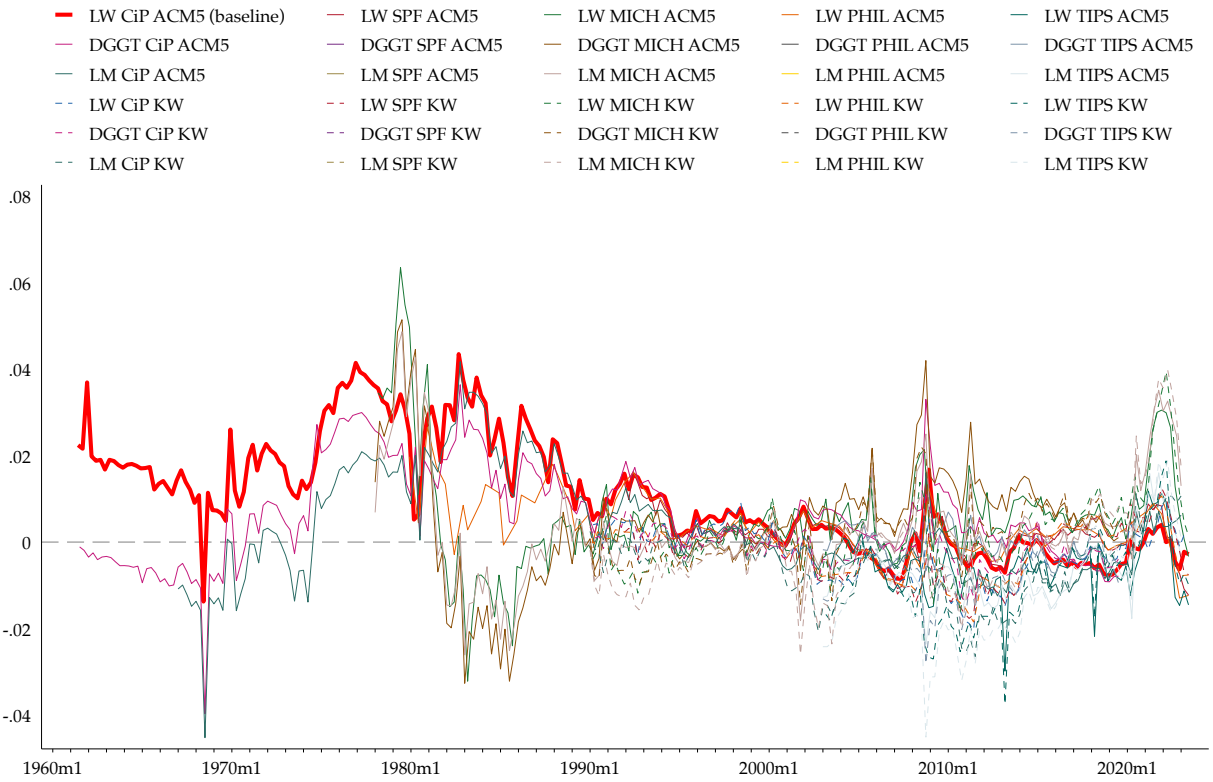


## 2.3. International evidence

We also sought evidence for or against the natural rate puzzle in 5 other advanced economies: Japan, Germany, the U.K., Canada, and Australia. Figure 3 presents these findings. For the real natural rate we use an established $r^*$ from an LW- or HLW-type model, the risk premium from an ACM-type estimation, inflation expectations from a CiP-type estimation, and the forward rate. However, established natural rate estimates of an LW- or HLW-type are only available for 6 out of our 10 sample countries, and so we cannot perform this exercise for France, Spain, Sweden, and Switzerland.

For the LW-type natural rate estimates we use the LW estimate itself for the U.S. as above; the Holston, Laubach, and Williams (2017) (two-sided estimates) for the Germany, U.K., and Canada; the Okazaki and Sudo (2018) (two-sided estimates) for Japan, and the McCririck and Rees (2017) (two-sided estimates) for Australia. We then replicate the ACM (3-factor) and CiP methodologies for these 6 countries and construct forward rates from zero-coupon bonds, as described later in this paper, and finally compute the discrepancy for all the countries to complete the analysis, with *discrepancy* = $RP - (f - r^* - \pi^*)$, as above.

**Figure 3:** *The natural rate puzzle in international data*

This chart displays the discrepancy in Equation 1 for the set of 6 countries. The presentation is based on Equation 1 and the series computed is *discrepancy* = $RP - (f - r^* - \pi^*)$, where RP is estimated using an ACM-style model. The sample is restricted to periods in which the full zero-coupon curve is available and an existing independent $r^*$ estimate is also available. See text.

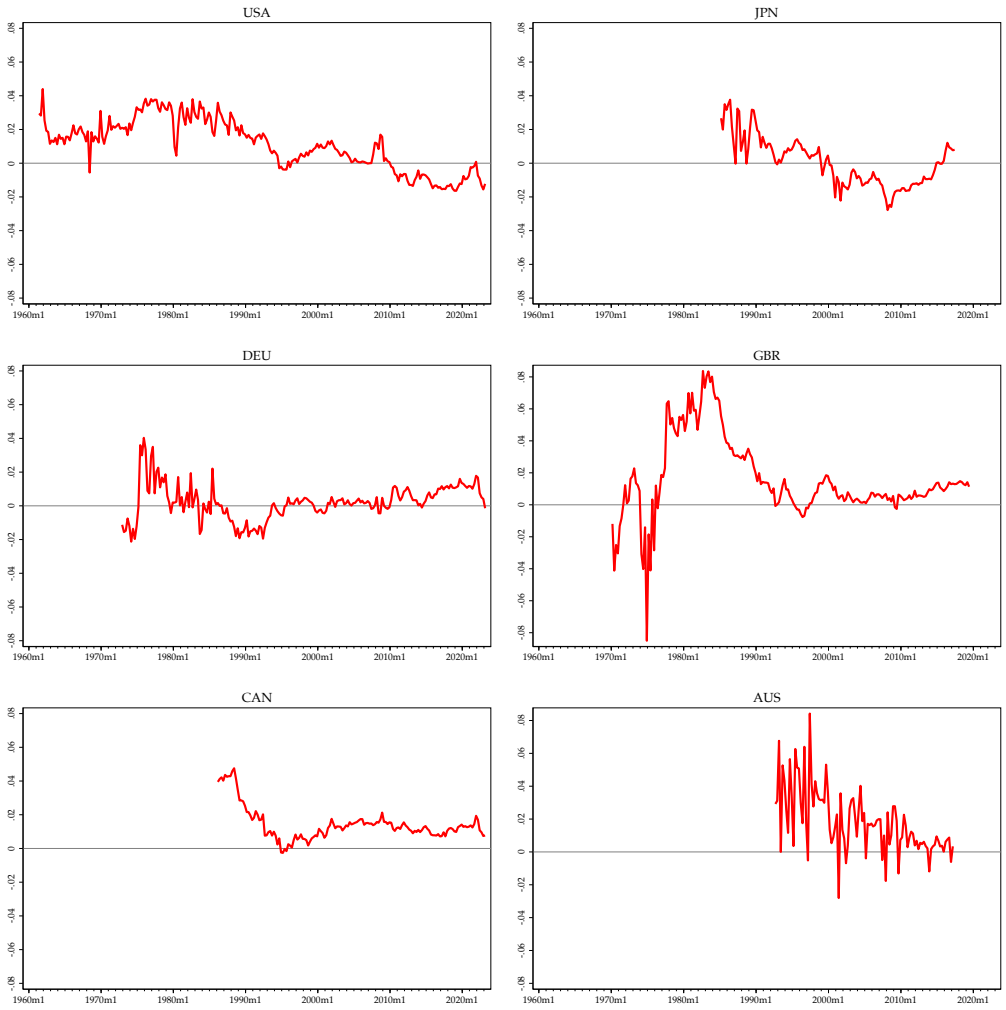


The discrepancy can be visualized over time in Figure 3, which presents the time-series data for each natural rate estimate. Here again, discrepancies of several hundred basis points are not uncommon. Germany shows the smallest discrepancy overall. In other cases the gap is typically positive and falling after 1980, indicating that the ACM risk premium estimates lie well above the implied estimates. In short, the natural rate puzzle is not simply a U.S. puzzle. It applies to many advanced economies, suggesting a deeper and more general pattern of conflict between widely-used standard estimates of the natural rate and bond risk premia.

## 3. Term-structure models with two macro factors

We use the 2-trend model of Cieslak and Povala (2015) which builds on the insights of Kozicki and Tinsley (2001). At time $t$, denote the nominal yield on an $n$-period bond by $y_t^{(n)}$, trend inflation by $\pi_t$, and the trend real natural rate by $r_t$. Yields across all maturities are driven by the trends and other factors contained in a price-of-risk factor $x_t$ vector, so the full set of factors is $F_t = (\pi_t, r_t, x_t)'$. In Cieslak and Povala (2015) $x_t = \bar{y}_t = \frac{1}{N}\sum_1^N y_t^{(n)}$ is 1-factor, and is the average yield across the curve.[1]

The short-rate process is assumed to depend on the factors, which in turn follow independent AR(1) processes, with

$$y_t^{(1)} = \delta_0 + \delta_\pi \pi_t + \delta_r r_t \,, \tag{2}$$

$$r_t = \mu_r + \phi_r r_{t-1} + \sigma_r \epsilon_t^r \,, \tag{3}$$

$$\pi_t = \mu_\pi + \phi_\pi \pi_{t-1} + \sigma_\pi \epsilon_t^\pi \,, \tag{4}$$

where $\delta_\pi > 0, \delta_r > 0$, with $\delta_x = 0$, as shown, and $\epsilon_t^\pi, \epsilon_t^r$ are standard normal, i.i.d.

At Equation 2, a natural benchmark is $\delta_0 = 0, \delta_\pi = \delta_r = 1$, i.e., the Fisher constraints. At Equation 3 and Equation 4, with persistent inflation we expect $\phi_\pi < 1$ but close to unity. The natural rate also tends to be persistent, with $\phi_r < 1$ and close to unity. Cieslak and Povala (2015) estimate annual $\hat{\phi}_\pi = 0.975$, $\hat{\phi}_r = 0.75$ for their U.S. sample.

The *endpoints* for the trends are the long-run limits (Kozicki and Tinsley, 2001). Allowing for possibly time-varying parameters the unconditional means of the endpoints are $r_\infty^{(t)} = \mu_r^{(t)}/(1-\phi_r^{(t)})$ and $\pi_\infty^{(t)} = \mu_\pi^{(t)}/(1-\phi_\pi^{(t)})$. These values prevail in the long run when all shocks have died out.

Finally, the price-of-risk factor follows an AR(1) process with i.i.d. normal shocks,

$$x_t = \mu_x + \phi_x x_{t-1} + \sigma_x \epsilon_t^x \,. \tag{5}$$

Cieslak and Povala (2015) estimate $\hat{\phi}_x = 0.392$ for the U.S. when detrending with the inflation trend.

The model economy is then compactly described by the equations

$$F_t = \mu + \Phi F_{t-1} + \Sigma \epsilon_t \,, \qquad y_t^{(1)} = \delta_0 + \delta_1' F_t \,, \tag{6}$$

with $\Phi$ and $\Sigma$ diagonal, $\delta_1 = (\delta_\pi, \delta_r, 0)'$, and $\epsilon_t = (\epsilon_t^\pi, \epsilon_t^r, \epsilon_t^x)'$.

**Detrended version** This is (see Duffee, 2011) a "yields-plus" model and not a "yields-only" model. That is, we are interested in whether the two macro trends $r_t$ and $\pi_t$ add useful information over and above a model using just a set of yield-based factors. To parse out the role of the trends

[1] This baseline setup is motivated by the Cochrane and Piazzesi (2005) finding that a single-factor can explain bond pricing quite well, but $x$ could be expanded to a vector as in three-factor yield models (Nelson and Siegel, 1987; Litterman and Scheinkman, 1991; Joslin, Singleton, and Zhu, 2011) or even five-factor yield models (Adrian, Crump, and Moench, 2015).

Cieslak and Povala (2015) reformulate the model using yields which have been *detrended*: define the detrended yield by $\bar{c}_t = \bar{y}_t - \bar{A}_n - \bar{B}_n^r r_t - \bar{B}_n^\pi \pi_t$ , which is the residual from the regression defined by Equation 10 for the average yield with the yield factor $x$ suppressed.

The model can then be expressed in our preferred form in terms of $x_t = \bar{c}_t$ and the full set of factors consists of the two trends and the detrended average yield, $F_t = (\pi_t, r_t, \bar{c}_t)'$. Now the unconditional mean of $F_t$ is now $\mu = E(F_t) = (\pi_\infty^{(t)}, r_\infty^{(t)}, 0)$. This reformulation leaves the model unchanged, but this attribution exercise reveals how yield factors are driven by the macro trends.

**Restricting the SDF** Using a standard no-arbitrage affine term-structure model as in Cieslak and Povala (2015), the log nominal stochastic discount factor is exponentially affine in the risk factors,

$$m_{t+1} = -y_t^{(1)} - \frac{1}{2}\Lambda_t'\Lambda_t - \Lambda_t'\epsilon_{t+1}\,, \tag{7}$$

where $\Lambda_t$ is the compensation for risk of shock $\epsilon_{t+1}$, with $\Lambda_t = \Sigma^{-1}(\lambda_0 + \Lambda_1 F_t)$.

We need more structure to make progress and the loadings in $\Lambda_t$ are assumed to take the form

$$\lambda_0 = \begin{pmatrix} \lambda_{0\pi} \\ \lambda_{0r} \\ 0 \end{pmatrix}, \qquad \Lambda_1 = \begin{pmatrix} 0 & 0 & \lambda_{\pi x} \\ 0 & 0 & \lambda_{rx} \\ 0 & 0 & 0 \end{pmatrix}. \tag{8}$$

As is seen in a wide range of established term structure models, the price of risk is assumed to follow a univariate process that is independent of other state variables. Cieslak and Povala (2015) estimate $\hat{\lambda}_{\pi x} = -0.47$ and $\hat{\lambda}_{rx} = 0.16$ for their U.S. sample.

**Solving the model** The model can then be solved (e.g., Duffee, 2013) as a set of affine equations for log bond prices, yields, forwards, and excess returns, in terms of the factors:

$$p_t^{(n)} = \mathcal{A}_n + \mathcal{B}_n' F_t\,, \tag{9}$$

$$y_t^{(n)} = A_n + B_n' F_t\,, \tag{10}$$

$$f_t^{(n,m)} = (\mathcal{A}_n - \mathcal{A}_{n+m}) + (\mathcal{B}_n - \mathcal{B}_{n+m})' F_t\,, \tag{11}$$

$$rx_{t+1}^{(n)} = \mathfrak{B}_n' F_t + v_t^n\,, \tag{12}$$

where $A_n = -\frac{1}{n}\mathcal{A}_n$, $B_n = -\frac{1}{n}\mathcal{B}_n$, $v_t^n = \mathcal{B}_{n-1}'\Sigma\epsilon_{t+1}$.

Solutions are derived from Riccati equations, where the recursions are

$$\mathcal{A}_{n+1} = -\delta_0 + \mathcal{A}_n + \mathcal{B}_n'\mu^q + \frac{1}{2}\mathcal{B}_n'\Sigma\Sigma'\mathcal{B}_n\,, \qquad \mathcal{B}_{n+1} = -\delta_1 + (\Phi^q)'\mathcal{B}_n\,, \tag{13}$$

with $\mathcal{A}_0 = 0$, $\mathcal{B}_0 = 0$, and risk-neutral dynamics governed by $\mu^q = \mu - \lambda_0$ and $\Phi^q = \Phi - \Lambda_1$.[2]

[2]The closed form solution for $\mathcal{B}_n$ is $\mathcal{B}_n = -\left[\sum_{j=0}^{n-1}(\Phi^q)^j\right]'\delta_1$.

Concretely, in the baseline model used here, factor loadings of bond prices can be derived as

$$\mathcal{B}_n^{\pi} = -\delta_{\pi}\frac{1-\phi_{\pi}^n}{1-\phi_{\pi}}, \qquad \mathcal{B}_n^{r} = -\delta_{r}\frac{1-\phi_{r}^n}{1-\phi_{r}}, \qquad \mathcal{B}_n^{x} = -\mathcal{B}_{n-1}^{\pi}\lambda_{\pi x} - \mathcal{B}_{n-1}^{r}\lambda_{rx} + \mathcal{B}_{n-1}^{x}\phi_x, \tag{14}$$

and the factor loadings of excess returns attach only to the price-of-risk factor, with

$$\mathfrak{B}_n = \mathcal{B}_{n-1}'(\lambda_0 + \Lambda_1 \mathbf{1}_3)x_t - \frac{1}{2}\mathcal{B}_{n-1}'\Sigma\Sigma'\mathcal{B}_{n-1}. \tag{15}$$

**Corollary 1: Long-dated forwards, macro trend endpoints, and the bond risk premium** The model we can provide justification for the decomposition at Equation 1 to introduce the natural rate puzzle.For a 1-period forward at horizon $n$, $f_t^{(n,1)} = (\mathcal{A}_n - \mathcal{A}_{n+1}) + (\mathcal{B}_n - \mathcal{B}_{n+1})'F_t$ and from the recursions (e.g., Duffee, 2013) we obtain

$$f_t^{(n,1)} = \underbrace{-\frac{1}{2}\mathcal{B}_{n-1}'\Sigma\Sigma'\mathcal{B}_{n-1}}_{\text{negative convexity term}} + \underbrace{\delta_0 - \mathcal{B}_n'\mu^q + \delta_1'(\Phi^q)^n F_t}_{\text{expected short rate under } q}. \tag{16}$$

Let the benchmark Fisher constraints hold, $\delta_0 = 0, \delta_\pi = \delta_r = 1$, substitute for $\mu_i$, and we have

$$\lim_{n\to\infty} f_t^{(n,1)} = \underbrace{r_\infty^{(t)}}_{\substack{\text{endpoint for}\\ \text{natural rate}}} + \underbrace{\pi_\infty^{(t)}}_{\substack{\text{endpoint for}\\ \text{inflation}}} + \underbrace{\mathcal{B}_\infty^{\pi}\lambda_{0\pi} + \mathcal{B}_\infty^{r}\lambda_{0r} - \frac{1}{2}\mathcal{B}_\infty'\Sigma\Sigma'\mathcal{B}_\infty}_{\text{bond risk premium as } n\to\infty}. \tag{17}$$

Thus, in this case, the limiting forward rate equals the sum of the natural rate and inflation endpoints and the limiting bond risk premium.[3] Intuitively, for small $n$ transitory variations in short-rate expectations matter due to the term $\delta_1'(\Phi^q)^n F_t$; in the limit for large $n$ these deviations fade away.

**Corollary 2: Expected returns and the cyclical factor** We can also show that the final term at Equation 17 also resembles a bond risk premium, as in Equation 1. From Equation 15 only the cyclical factor $x_t = \bar{c}_t$ predicts bond excess returns, and not the trends themselves,

$$rx_{t+1}^{(n)} = \mathcal{B}_{n-1}'(\lambda_0 + \Lambda_1 F_t) - \frac{1}{2}\mathcal{B}_{n-1}'\Sigma\Sigma'\mathcal{B}_{n-1} + \mathcal{B}_{n-1}'\Sigma\epsilon_{t+1}. \tag{18}$$

Of course, this does *not* mean than shifts in $r_t$ and $\pi_t$ play no role: they will of course change the cyclical deviation $x_t = \bar{c}_t$ via detrending. Now setting $x_t = \bar{c}_t$, we have in the limit

$$\lim_{n\to\infty} E_t(rx_{t+1}^{(n)}) = \underbrace{(\mathcal{B}_\infty^{\pi}, \mathcal{B}_\infty^{r})'(\Lambda_{\pi x}\bar{c}_t, \Lambda_{rx}\bar{c}_t)}_{\text{cyclical price-of-risk factor terms}} + \underbrace{\mathcal{B}_\infty^{\pi}\lambda_{0\pi} + \mathcal{B}_\infty^{r}\lambda_{0r} - \frac{1}{2}\mathcal{B}_\infty'\Sigma\Sigma'\mathcal{B}_\infty}_{\text{bond risk premium as } n\to\infty}. \tag{19}$$

For large $n$ the two risk premia terms (the last terms) in Equation 17 and Equation 19 are the same.

[3] As $n \to \infty$, $\mathcal{B}_n^{\pi} \to -\pi_\infty^{(t)}/\mu_\pi$, $\mathcal{B}_n^{r} \to -r_\infty^{(t)}/\mu_r$, and $(1-\phi_x)\mathcal{B}_n^{x} \to \lambda_{\pi x}\pi_\infty^{(t)}/\mu_\pi + \lambda_{rx}r_\infty^{(t)}/\mu_r$, with $\mu_c = 0$.

## 4. Reduced-form model estimation and model evaluation

Guided by the above structural model, we operationalize it via the following Bayesian reduced-form estimation method, as in common. We restore the star notation, and denote by $r_t^*$ the trend natural rate, and by $\pi_t^*$ trend inflation.

On the "finance-side" of the model, we aim to extract the latent $r_t^*$ from average bond yields by using state-space estimation with an affine measurement equation of the form

$$\bar{y}_t = a_y + b_\pi \pi_t^* + b_r r_t^* + \epsilon_t^{cyc} \,, \tag{20}$$

where $\pi_t^*$ is trend inflation, treated as an observable, and set equal to the Cieslak and Povala (2015) constant-gain learning measure. This equation can be seen as deriving from the structural Equation 10 with $y_t^{(n)} = A_n + B_n' F_t$ averaged over all maturities, 1 to 180 months. [4] Here, note that the risk factor $x_t = \bar{c}_t$ and its disturbance terms are absorbed into the "cyclical" error term $\epsilon_t^{cyc}$, and we assume that the error term follows an AR(1) processes of the form

$$\epsilon_{t+1}^{cyc} = \rho_y \epsilon_t^{cyc} + e_{t+1}^{cyc} \,, \qquad e_{t+1}^{cyc} \sim N(0, \sigma_{cyc}^2) \,. \tag{21}$$

We turn to the "macro-side" of the model. Let $g_t$ denote trend real GDP growth. We also treat this variable as observable conditional on time $t$, set equal to the as-of-date, rolling, exogenously detrended rate of real GDP growth using a one-sided Hodrick-Prescott filter. We then define the state variable $z_t$ as a "headwinds" factor related to the natural rate through the state transition equation

$$r_t^* = z_t + g_t \,, \tag{22}$$

as is standard in state-space models of the natural rate, such as Laubach and Williams (2003), with the coefficient on growth set to unity. Finally, we also assume that the headwinds factor follows an AR(1) process, so that

$$z_{t+1} = \rho_z z_t + e_{t+1}^z \,, \qquad e_{t+1}^z \sim N(0, \sigma_z^2) \,. \tag{23}$$

Again, we stress why we we see this not just as a macro-finance model, but also the minimal such model we could set up that contains both yields and macro data. The key finance part is the underlying term-structure model of the yield curve. The key macro part is $r^* = z + g$, which derives its meaning from the constraints put on $z$ and is disciplined through our prior assumptions on its process, in particular its prior volatility. This will allow us to generate a path for $r^*$, tied in to both the macro and finance blocks, but with little theoretical baggage otherwise.

Consistent with the relative frequencies of financial series and macroeconomic series, the headwinds factor, $z_{t+1}$, is conjectured to capture structural macroeconomic phenomena with a frequency similar to that of macroeconomic series, while the error to average yields, $\epsilon_{t+1}^{cyc}$, is assumed

[4] One could entertain model variants with more points across the curve, but they are more difficult to estimate without more structure, since for each point they add one equation and at least four more parameters.

to capture high frequency movements from financial phenomena. Through Equation 22 this implies a view of the natural rate $r_t^*$ consistent with Laubach and Williams (2003) of representing a medium-run real rate "anchor" for monetary policy. In Appendix A we provide details on how explicit identification assumptions about $\rho_z$ and $\sigma_z$ prevent the headwinds variable from taking a high frequency similar to that of financial prices. We use priors to impose this view on variable volatility, without explicitly linking the headwinds factor to a particular set of low frequency structural data. We use a common prior structure across all countries to restrict the degrees of freedom and to reflect the view that the underlying model, and particularly the drivers of the natural rate of interest, should be similar across countries.

Summarizing, the Kalman system is thus defined by the following state equation,

$$\begin{pmatrix} z_t \\ \epsilon_t^{cyc} \end{pmatrix} = \begin{pmatrix} \rho_z & 0 \\ 0 & \rho_{cyc} \end{pmatrix} \begin{pmatrix} z_{t-1} \\ \epsilon_{t-1}^{cyc} \end{pmatrix} + \begin{pmatrix} e_t^z \\ e_t^{cyc} \end{pmatrix}. \tag{24}$$

The associated measurement equation can then be written as

$$\overline{y}_t = a_y + b_\pi \pi_t^* + b_{r^*} g_t + b_{r^*} z_t + \epsilon_t^{cyc}. \tag{25}$$

This fully describes the state-space model, which has then to be estimated. The estimation algorithm is described in Appendix A.

## 5. Data for estimation and evaluation

Estimation and model evaluation lead us to collect bond data for 10 advanced countries over the postwar period. The data requirements are as follows, and prompted us to collect data over two different windows, a broad window and a narrow window.

**Estimation and evaluation: narrow window using full zero-coupon curves** Estimation usesthe equation $\overline{y}_t = a_y + b_\pi \pi_t^* + b_{r^*} g_t + b_{r^*} z_t + \epsilon_t^{cyc}$. In samples where we have complete information on the zero-coupon yield curve we can construct a true average yield based on 1 to 15 year maturity zero-coupon yields. We also need the more easily sourced data on the rate of output growth ($g_t$) and the inflation trend ($\pi_t^*$, computed via constant-gain learning),.

We refer to these samples as the *narrow window*, and to evaluate the model we fit equations for yields and returns, $y_t^{(n)} = A_n + B_n' F_t$ and $rx_{t+1}^{(n)} = \mathfrak{B}_n' F_t + v_t^n$. Specifically we model yields (at 10 years) and excess returns (averaged over maturities 2 to 180 months, with inverse-maturity weights).

**Estimation and evaluation: broad window using proxy average yields** Estimation uses the measurement affine equation $\overline{y}_t = a_y + b_\pi \pi_t^* + b_{r^*} g_t + b_{r^*} z_t + \epsilon_t^{cyc}$. Given data on the rate of output growth and the inflation trend, this step can still be carried through in samples where we have an acceptable proxy of average yields, and we lack the full zero-coupon yield curve.

We refer to these samples as the *broad window*, where we can still achieve an estimate of the latent natural rate $r_t^*$. Also in this case to evaluate the model we can still examine the fit of the affine equations for excess returns, $rx_{t+1}^{(n)} = \mathfrak{B}_n' F_t + v_t^n$, but without the zero-coupon yield curve we need to rely on a proxy measure of excess returns as detailed below.

Whilst the broad window method may give less precise estimates of the natural rate, we find strong correlations between our proxies for yields and returns and their values computed using complete information on the zero-coupon yield curve where the methods overlap in the narrow window. Still, one virtue is that we can compute natural rates often for an extra 10 or 20 years going back to the 1950s and 1960s for the countries in our sample. A second important virtue is that the longer samples provided by this proxy method allow us to achieve more stable estimates of the latent variables by the time the starting point of the narrow window is reached, pushing back the period of initialization where the filter can produce unstable and unreliable estimates (we typically drop the first 5 years a a burn-in period in results shown below).

**Data: narrow window** In the narrow window samples we need the full zero-coupon yield curve. We rely here on existing datasets by official institutions and other researchers. We obtain the curves from a Nelson-Siegel-Svensson Nelson and Siegel (1987); Svensson (1994) model, where the set of time-varying parameters $\beta_{0,t}, \beta_{1,t}, \beta_{2,t}, \beta_{3,t}, \tau_{1,t}$, and $\tau_{2,t}$ are estimated to express the smoothly-approximated yield $y_t^{(n)}$, at any given time $t$, of a maturity $n$ zero-coupon bond as

$$y_t^{(n)} = \beta_{0,t} + \beta_{1,t} \frac{1 - e^{-n/\tau_{1,t}}}{n/\tau_{1,t}} + \beta_{2,t} \left( \frac{1 - e^{-n/\tau_{1,t}}}{n/\tau_{1,t}} - e^{-n/\tau_{1,t}} \right) + \beta_{3,t} \left( \frac{1 - e^{-n/\tau_{2,t}}}{n/\tau_{2,t}} - e^{-n/\tau_{2,t}} \right). \quad (26)$$

Obtaining the parameters of a Svensson model lets us generate zero-coupon yields for all maturities from 1 to 360 months at each point in time, circumventing the problem of data sparsity in some parts of the curve. For some countries, the datasets by official institutions and other researchers already provide estimates of the above parameters; we can then directly compute the curve without any further step. In other cases, the datasets available to us consist of zero-coupon yields at a large number (but maybe not all) maturities, and possibly built from alternative models; in these cases we simply fit a Nelson-Siegel-Svensson (NSS) curve as a preliminary step at each date.

For the 10 countries our sources for these monthly fitted NSS zero-coupon yield curves are as follows, and in the current paper the sample end date is June 2023:

- U.S.: parameters from Gürkaynak, Sack, and Wright (2007) and updates, from June 1961.
- Japan: parameters estimated from the prices, coupons, and maturities of individual bonds quoted on Datastream.[5]
- Germany: parameters from the Bundesbank from October 1972.

[5]We elected not to employ the widely-used Ministry of Finance curve starting in September 1974, as it is a coupon curve. So we reconstructed the zero curve from scratch.

- U.K.: Bank of England data on yields for maturities ranging from 0.5 years to 25 or 40 years, allowing us to recover parameters from January 1970.
- Canada: Bank of Canada data on yields for maturities ranging from 0.25 years to 30 years, allowing us to recover parameters from January 1986.
- Australia: Reserve Bank of Australia data on yields from 0 to 10 years in quarterly maturity increments, allowing us to recover parameters from July 1992.
- France: up to 2004 curves kindly supplied by Cadorel (2022), at maturities from 1 to 40 years; from 2005, curves at maturities from 1 to 50 years, from Grishchenko, Moraux, and Pakulyak (2020) and subsequent updates; we recover parameters from December 1944, with the gap in a few recent months constructed manually from Bloomberg.
- Spain: parameters kindly supplied by the BIS to construct yield curves from January 1991, with the gap in a few recent months constructed manually from Bloomberg.
- Sweden: parameters from the Riksbank from December 1992.
- Switzerland: parameters from the Swiss National Bank from January 1988.

To the best of our knowledge, this compilation provides a new and unique set of zero-coupon data by extending a consistent methodology to other advanced economies and over many more years.[6]

**Data: broad window** The availability of complete zero-coupon yield curves varies. We have full coverage for all 10 countries in the last three decades, since roughly the early 1990s. Before that only a handful of countries can be covered.

As noted, we can use proxies ($\tilde{y}_t$ and $\tilde{y}_t^{(1)}$) to approximate average yields and short rates, and given those proxies, and without a curve, we can approximate average excess bond returns ($\widetilde{rx}_t = \tilde{y}_t - k\tilde{y}_{t+1} - (1-k)y_t^{(1)}$), where the average is over bonds of maturities from 2 to 15 years.[7]

We therefore rely on an array of secondary sources for proxy average yields and short rates. These will typically reference an average built from a vaguely defined basket of long bonds, or will present a time series of multiple long bond yields from which we can mechanically construct an average. Sources used here include technical documents from central banks and finance ministries, or from the OECD, and aggregators such as Global Financial Data and Haver.

[6]The closest prior work was a decade ago. Wright (2011) compiled a 10-country panel of zero-coupon yields with the data series ending in 2009, using Svensson, Nelson-Siegel, and spline models.

[7]Consider an inverse-duration weight basket of bonds at annual maturity increments $n = 2, \ldots, 15$. The forward excess return of the maturity $n$ bond is $ny_t^{(n)} - (n-1)y_{t+1}^{(n-1)} - y_t^{(1)}$. Applying a weight $1/n$ and summing over all 14 bonds we obtain a weighted average return $\overline{rx}_t = \frac{1}{14}\sum_{n=2}^{15} y_t^{(n)} - \frac{1}{14}\sum_{n=2}^{15}\frac{(n-1)}{n}y_{t+1}^{(n-1)} - \frac{1}{14}\sum_{n=2}^{15}\frac{1}{n}y_t^{(1)}$. We take the approximation to this given by $\widetilde{rx}_t = \tilde{y}_t - \left(\frac{1}{14}\sum_{n=2}^{15}\frac{(n-1)}{n}\right)\tilde{y}_{t+1} - \left(\frac{1}{14}\sum_{n=2}^{15}\frac{1}{n}\right)y_t^{(1)}$. Now define $k \equiv \left(\frac{1}{14}\sum_{n=2}^{15}\frac{(n-1)}{n}\right)$ and we can write $\widetilde{rx}_t = \tilde{y}_t - k\tilde{y}_{t+1} - (1-k)y_t^{(1)}$.

## 6. Estimates and fit of yield and return equations

In this subsection, we now apply the affine model with OLS regressions based on Equation 10, $y_t^{(n)} = \mathcal{A}_n + \mathcal{B}_n^r r_t^* + \mathcal{B}_n^\pi \pi_t^* + \mathcal{B}^{\bar{c}} \bar{c}_t$. This is the specification in Cieslak and Povala (2015), but with a second trend for the estimated natural rate. The detrended average yield $\bar{c}_t$ then represents a cyclical (high-frequency) fluctuation of bond yields (or prices) about the long-run trends. We could also run this regression in equivalent form with $\bar{c}_t$ replaced by $\bar{y}_t$, but this would only produce different coefficients, a different interpretation or attribution, but the model and fit would be the same.

Table 1 presents OLS yield regressions at the 10-year maturity point. Results at other maturities are similar but not shown. We expect loadings on all factors to be positive and under the Fisher conditions, close to 1. This is true for the full sample, with the exclusion of Spain, in panel (a). Once we exclude the GFC period, 2007 and later, in panel (b) all loadings are positive including the coefficients for Spain. This exception makes sense, however: during the Eurozone crisis yields in Spain rose due to default risk while growth and the natural rate collapsed. The model is designed to price safe Treasury bonds, and this period in Spain would violate that assumption.

Of great interest, as highlighted by Cieslak and Povala (2015), is the role of the trends versus the detrended yield term in accounting for the fit. If we exclude each trend one at a time then the importance of the trends becomes clear. First, adding the inflation trend improves the fit of the yield model relative to a specification with no trends. Second, adding the natural rate trend improves the fit even more, so both trends are relevant for bond pricing (Bauer and Rudebusch, 2020).

This key role of the trends is shown in Figure 4, where the Shapley decomposition of $R^2$ shows that with overall fit close to 0.99, most of that fit, between 0.8 and 0.95, is attributable to the two macro trends. In other words, rather than yield pricing being mostly down to a pure high-frequency level factor, it is instead a combination of highly influential but slow-moving macro trends in $r_t^*$ and $\pi_t^*$, and a small residual cyclical component that explains the residual variation.

Finally, for more perspective, Table 2 looks at the performance of the above macro trend model of yields as compared to models based on principal components. The table reports the pooled root mean square error (RMSE) for 10 country-level yield regressions on the same full sample reported in Table 1. The models considered are the Null model (constant term only), the models based on 0-1-2 macro trends, and models based on 1-2-3 principal components of the cross-section of yields (e.g. Adrian, Crump, and Moench, 2013). The macro trends do not add much to the fit, but change the attribution of the fit. And all of the trend models perform better than the PC1 model, and slightly better than PC2. However, using three principal components does better still, as is well known, since level, slope and curvature all contain useful information for fitting different points on the curve, and the PC123 model does a good job of spanning that information, where the macro trends clearly cannot bring in the additional information embedded in PC3.

To reiterate, the macro trend model performs well as a model of yields as judge by fit, but all yield models fit with very high $R^2$ and the macro trend model does not have as full a set of information about yields as models based on 3 or more principal components of yields.

**Table 1:** *International yields affine model for 10-year maturity*

The tables reports OLS estimates on international monthly data of 10-year yields $y_t^{(n)} = \tilde{\mathcal{A}}_n + \tilde{\mathcal{B}}^{\bar{c}} \bar{c}_t$, with $n = 120$ months. The sample varies by country. Standard errors are corrected for estimation error in the natural rate using a wild block bootstrap with 1,000 draws. See text.

| **(a) Narrow window dataset, full sample. Detrending: $\bar{c}$ equal to projection of $\bar{y}$ on $\pi^*$ and $r^*$** | | | | | | | | | | |
|---|---|---|---|---|---|---|---|---|---|---|
| | AUS | CAN | CHE | DEU | ESP | FRA | GBR | JPN | SWE | USA |
| $r^*$ | 1.161 | 1.075 | 1.130 | 1.194 | -0.323 | 1.219 | 1.539 | 0.679 | 1.927 | 1.018 |
| | (0.116) | (0.077) | (0.115) | (0.092) | (0.035) | (2.701) | (0.141) | (0.096) | (0.241) | (0.120) |
| $\pi^*$ | 1.039 | 0.904 | 0.979 | 0.802 | 1.852 | 0.962 | 0.756 | 0.768 | 1.252 | 1.017 |
| | (0.076) | (0.099) | (0.115) | (0.086) | (0.028) | (0.025) | (0.058) | (0.104) | (0.085) | (0.080) |
| $\bar{c}$ | 0.945 | 0.906 | 0.803 | 0.856 | 1.042 | 0.902 | 0.990 | 0.905 | 0.983 | 0.895 |
| | (0.010) | (0.013) | (0.014) | (0.010) | (0.010) | (0.018) | (0.010) | (0.023) | (0.008) | (0.011) |
| Constant | -0.006 | -0.001 | -0.001 | 0.002 | -0.005 | -0.002 | -0.005 | 0.001 | -0.021 | 0.000 |
| | (0.005) | (0.002) | (0.002) | (0.002) | (0.001) | (0.004) | (0.003) | (0.001) | (0.010) | (0.002) |
| Observations | 372 | 450 | 426 | 609 | 391 | 641 | 642 | 523 | 367 | 712 |
| $R^2$ | 0.997 | 0.996 | 0.995 | 0.995 | 0.996 | 0.989 | 0.996 | 0.996 | 0.997 | 0.994 |
| RSS | 0.0007 | 0.0016 | 0.0008 | 0.0026 | 0.0014 | 0.0089 | 0.0045 | 0.0018 | 0.0008 | 0.0038 |

| **(b) Narrow window dataset, sample ends 2006m12. Detrending: $\bar{c}$ equal to projection of $\bar{y}$ on $\pi^*$ and $r^*$** | | | | | | | | | | |
|---|---|---|---|---|---|---|---|---|---|---|
| | AUS | CAN | CHE | DEU | ESP | FRA | GBR | JPN | SWE | USA |
| $r^*$ | 1.416 | 1.190 | 2.698 | 1.257 | 0.595 | 1.665 | 0.843 | 0.658 | 0.660 | 1.010 |
| | (0.163) | (0.099) | (0.780) | (0.103) | (0.081) | (5.586) | (0.140) | (0.097) | (0.045) | (0.169) |
| $\pi^*$ | 0.934 | 0.898 | 0.999 | 0.831 | 1.640 | 1.069 | 0.736 | 0.786 | 1.161 | 1.016 |
| | (0.096) | (0.110) | (0.321) | (0.087) | (0.055) | (0.055) | (0.027) | (0.116) | (0.024) | (0.049) |
| $\bar{c}$ | 0.964 | 0.906 | 0.972 | 0.846 | 0.978 | 0.845 | 1.000 | 0.941 | 0.972 | 0.890 |
| | (0.014) | (0.017) | (0.022) | (0.012) | (0.011) | (0.022) | (0.012) | (0.023) | (0.012) | (0.010) |
| Constant | -0.013 | -0.005 | -0.031 | -0.002 | -0.022 | -0.019 | 0.017 | 0.001 | 0.012 | 0.000 |
| | (0.004) | (0.002) | (0.022) | (0.003) | (0.001) | (0.022) | (0.006) | (0.002) | (0.002) | (0.003) |
| Observations | 174 | 252 | 228 | 411 | 193 | 443 | 444 | 325 | 169 | 514 |
| $R^2$ | 0.994 | 0.992 | 0.991 | 0.987 | 0.997 | 0.980 | 0.992 | 0.995 | 0.996 | 0.992 |
| RSS | 0.0003 | 0.0009 | 0.0003 | 0.0018 | 0.0004 | 0.0071 | 0.0034 | 0.0011 | 0.0003 | 0.0022 |

**Table 2:** *International yields affine models: macro trends versus principal components*

The table reports the pooled root mean square error (RMSE) for 10 country-level yield regressions on the same full sample reported in Table 1. The models considered are the Null model (constant term only), the models based on 0-1-2 macro trends, and models based on 1-2-3 principal components of the cross-section of yields (e.g. Adrian, Crump, and Moench, 2013). See text.

| | Null | 0 trend | 1 trend | 2 trend | PC1 | PC12 | PC123 |
|---|---|---|---|---|---|---|---|
| RMSE | 0.0308 | 0.0024 | 0.0024 | 0.0023 | 0.0047 | 0.0026 | 0.0007 |
| $N$ | 5133 | | | | | | |

**Figure 4:** *Decomposition of in-sample fit: yield regressions with 0, 1, and 2 macro trends*

The chart displays $R^2$ values for the excess returns regressions by country. 0 denotes the model with no trend, 1 the model with $\pi^*$ trend, and 2 the model with $\pi^*$ and $r^*$ trends.

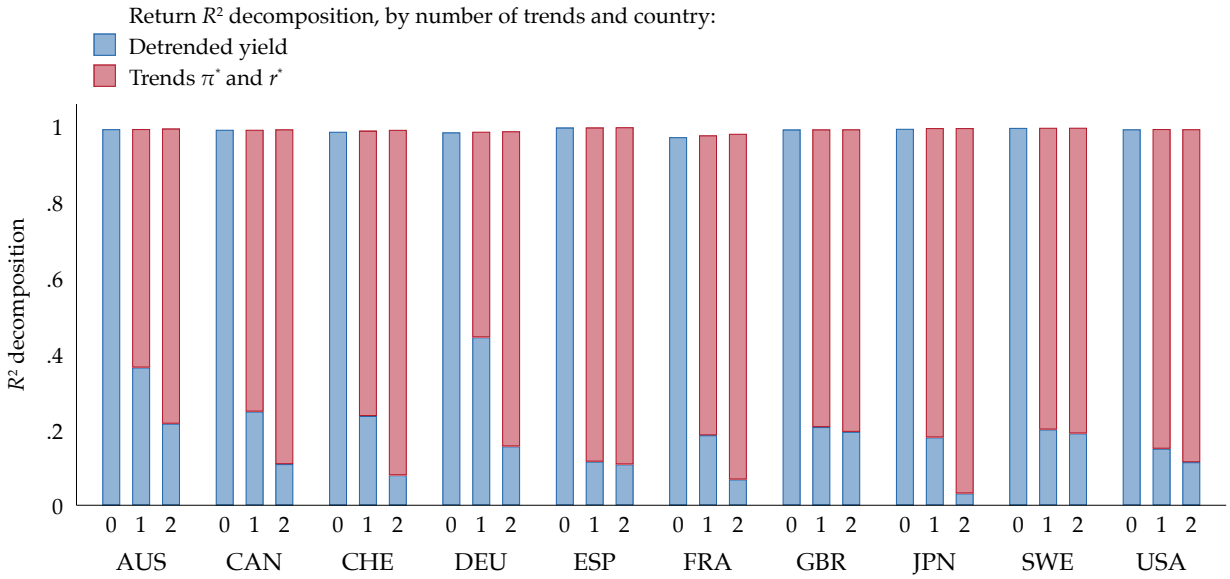


We now present estimates for the excess return Equation 12, $rx_{t+1}^{(n)} = \mathfrak{B}_n^\top F_t + v_t^n$. These one-step ahead predictions are noisy but their explanatory power is almost entirely due to the role of the detrended, or cyclical, yield factor $\bar{c}$. This is inline with the model and intuition, since the cyclical factor is the only driver of excess returns as we saw at Equation 19.

Table 3 present results for the excess return forecasts in the narrow window full sample. Here we have full zero-coupon yield curves and do not have to rely on proxy yields or proxy returns. Note that these are in-sample regressions (using 2-sided $r^*$ estimates from a Kalman filter run on full-sample data), so they do not speak to out of sample performance.

The model performs as expected in general. Loading on the two trends are typically small and generally not statistically significant based on the wild block bootstrap standard errors. Table 4 looks at the performance of the macro trend model of excess returns as compared to models based on principal components again judged by RMSE. Here fit is always poor in return forecasts, with a null RMSE of 91 bps being reduced to at best 81 bps in the 2-trend model. This reduction is still a big improvement in fit compared to that achieved by the 0 and 1 trend models, and does better than any of the principal components model up to PC123. Recall that the excess return here is on an average inverse-maturity weighted portfolio from 1 to 10 years. It appears that averaging along the curve in this case means that the extra information in the 3rd principal component, or curvature, is of less value, and the macro 2-trend model can here perform as well or better than its rivals.

**Table 3:** *International excess returns, affine model for an average inverse-maturity weighted portfolio*

The table reports OLS estimates on international data of the excess return equation $\overline{rx}_{t+1} = \mathfrak{B}_n^\top F_t + v_t^n$, where the bar denotes an average inverse-maturity weighted portfolio return. The sample varies by country. Standard errors are corrected for estimation error in the natural rate using a wild block bootstrap with 1,000 draws. See text.

| | (1) AUS | (2) CAN | (3) CHE | (4) DEU | (5) ESP | (6) FRA | (7) GBR | (8) JPN | (9) SWE | (10) USA |
|---|---|---|---|---|---|---|---|---|---|---|
| $r^*$ | -0.020 | 0.140 | 0.084 | -0.002 | 0.051 | 0.150 | -0.025 | 0.033 | 0.271 | 0.000 |
| | (0.097) | (0.054) | (0.074) | (0.045) | (0.070) | (1.092) | (0.054) | (0.056) | (0.137) | (0.081) |
| $\pi^*$ | 0.278 | -0.133 | -0.039 | 0.065 | 0.064 | -0.053 | 0.020 | 0.055 | 0.013 | -0.003 |
| | (0.078) | (0.064) | (0.059) | (0.045) | (0.048) | (0.015) | (0.017) | (0.060) | (0.054) | (0.049) |
| $\bar{c}$ | 0.692 | 0.555 | 0.293 | 0.339 | 0.729 | 0.398 | 0.220 | 0.471 | 0.499 | 0.520 |
| | (0.055) | (0.049) | (0.062) | (0.047) | (0.049) | (0.046) | (0.031) | (0.053) | (0.046) | (0.043) |
| Constant | -0.004 | 0.003 | 0.001 | 0.002 | 0.002 | 0.001 | 0.002 | 0.002 | -0.001 | 0.002 |
| | (0.004) | (0.001) | (0.001) | (0.001) | (0.001) | (0.002) | (0.001) | (0.001) | (0.005) | (0.001) |
| Observations | 361 | 439 | 415 | 598 | 380 | 630 | 631 | 512 | 356 | 701 |
| $R^2$ | 0.342 | 0.303 | 0.054 | 0.097 | 0.390 | 0.161 | 0.073 | 0.216 | 0.294 | 0.187 |
| RSS | 0.0196 | 0.0177 | 0.0174 | 0.0410 | 0.0274 | 0.0511 | 0.0649 | 0.0127 | 0.0220 | 0.0568 |

**Table 4:** *International excess return affine models: macro trends versus principal components*

The table reports the pooled root mean square error (RMSE) for 10 country-level excess return regressions on the same full sample reported in Table 1. The models considered are the Null model (constant term only), the models based on 0-1-2 macro trends, and models based on 1-2-3 principal components of the cross-section of yields (e.g. Adrian, Crump, and Moench, 2013). See text.

| | Null | 0 trend | 1 trend | 2 trend | PC1 | PC12 | PC123 |
|---|---|---|---|---|---|---|---|
| RMSE | 0.0091 | 0.0089 | 0.0085 | 0.0081 | 0.0089 | 0.0083 | 0.0083 |
| $N$ | 5023 | | | | | | |

## 7. Assessing the natural rate trends in 10 advanced economies

We now turn to a discussion of the macro trends, and especially our model estimates of the natural rate, the latent $r^*$ time series, which we obtain for all 10 countries. These estimates are displayed in **??**. Again we stress that prior work has not been able to generate a natural rate estimate for as many countries over as long a period in the postwar period, but we can still discuss the relevance and plausibility of these estimates as compared to prior consensus views and also by direct comparisons in places of overlap with other estimates. In this section we now discuss these comparisons, before moving on to evaluate how well our estimates conform with the drivers most commonly associated with the decline in $r^*$, namely slowing economic growth and demographic aging.

## 7.1. Comparison with HLW and other estimates

As we have noted, for cross-country estimates, Holston, Laubach, and Williams (2017) [HLW] is the earliest, best-known, and most widely-used precursor of our work, a study which provided natural rate estimates for 4 countries. So as a sense check we compare our estimates to HLW for the U.S., U.K., Canada, and the Euro Area (which we compare to our series for Germany, France, and Spain). HLW's estimates were suspended during the pandemic but have resumed, although not for the U.K.

In Figure 5 we see that our U.S. natural rate series is close the the HLW series in shape but is in general at a lower level. In the 1970s and again in the 2000s, our estimate is about 100–200 bps lower and towards the end of the sample our estimate is much closer to zero. In the Euro Area, our series shows more of a rise and fall pattern, and generally finds a much steeper decline after the 1990s, with natural rates turning negative in France and especially Germany, while the HLW series remains positive. For the U.K., we see an upswing and very large downswing in natural rates in the 1990s and afterwards, and our estimate is first higher and then drops lower, and close to zero at the end, about 150 bps below the HLW estimate. A similar pattern is seen for the case of Canada, but with our estimates also much lower earlier in the sample. We surmise that our estimates differ from HLW because we use information from the bond market at the longer end curve (via $\bar{y}$), so our different trends may arise as substantial variations in the headwinds $z$ could be apparent in longer-maturity bonds, with larger shifts in average yields than are implied from a model linked to GDP growth and short rates alone.

In Figure 6 we take comparisons much further and utilize all of the current natural rate estimates that we could find for all 10 of the countries in our sample. From this exercise we conclude that our estimates are not wildly out of line with previous work, but there are some notable difference in amplitude and timing. The other estimates are, in addition to HLW, as follows:

- GJST = Grimm, Jordà, Schularick, and Taylor (2023) for all 10 countries;
- DGGT = Del Negro, Giannone, Giannoni, and Tambalotti (2017) for USA and Del Negro, Giannone, Giannoni, and Tambalotti (2019) for 6 others;
- LM = Lubik and Matthes (2015) for USA;
- BOJ = Okazaki and Sudo (2018) for JPN; and
- RBA = McCririck and Rees (2017) for AUS.

In general, our estimates suggest that the decline in natural rates over the last 50 years has been somewhat larger in terms amplitude and somewhat later in terms of timing, as compared to other estimates. In almost all cases, we find the sharpest declines do not really commence until around the 1995–2005 window, with the exception of Japan where, as is well understood, the downswing had begun much earlier. In Europe, the trends in Germany and Spain begin the decline earlier than others, but for other European countries the main shift starts a bit later, and the peak is maybe even later still in Britain and the three New World economies.

**Figure 5:** *Trends in $r^*$, our estimates versus HLW*

The charts display the four HLW estimates of the natural rate $r^*$ and our 2-sided estimates.

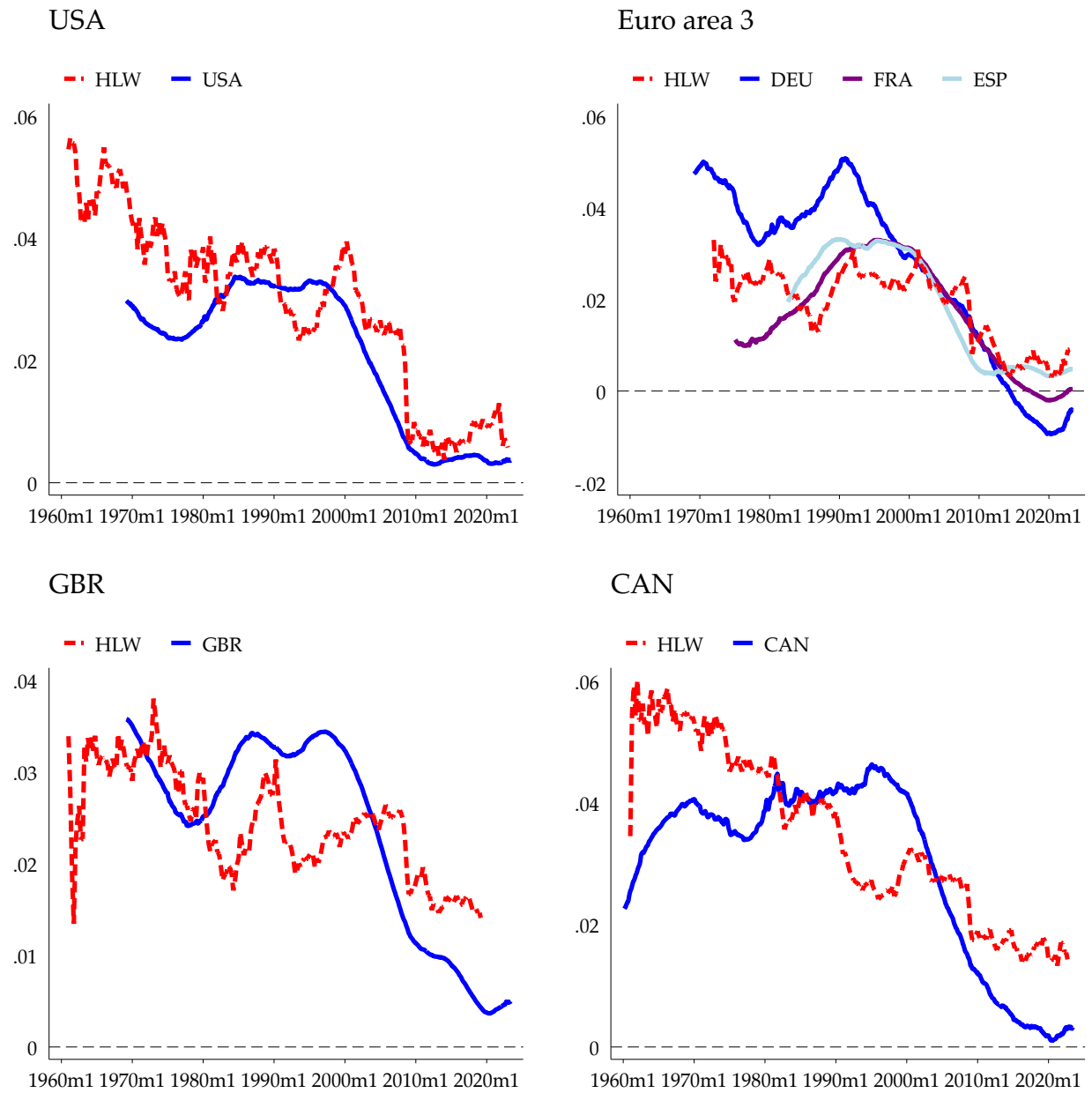

**Figure 6:** *Trends in $r^*$, our estimates versus other estimates*

The charts display various estimates of the natural rate $r^*$ and our estimates. Our estimates are shown in both 2-sided (solid line) and 1-sided (dashed line) forms. Other estimates are shown as a scatter using the following abbreviations in the legends: GJST = Grimm, Jordà, Schularick, and Taylor (2023); DGGT = Del Negro, Giannone, Giannoni, and Tambalotti (2017) for USA and Del Negro, Giannone, Giannoni, and Tambalotti (2019) for others; HLW = Holston, Laubach, and Williams (2017); LM = Lubik and Matthes (2015); BOJ = Okazaki and Sudo (2018); RBA = McCririck and Rees (2017). For reference, we also show trend growth $g$. A 95% posterior interval is shown around the 2-sided $r^*$ based on the s.d. of 2,000 draws.

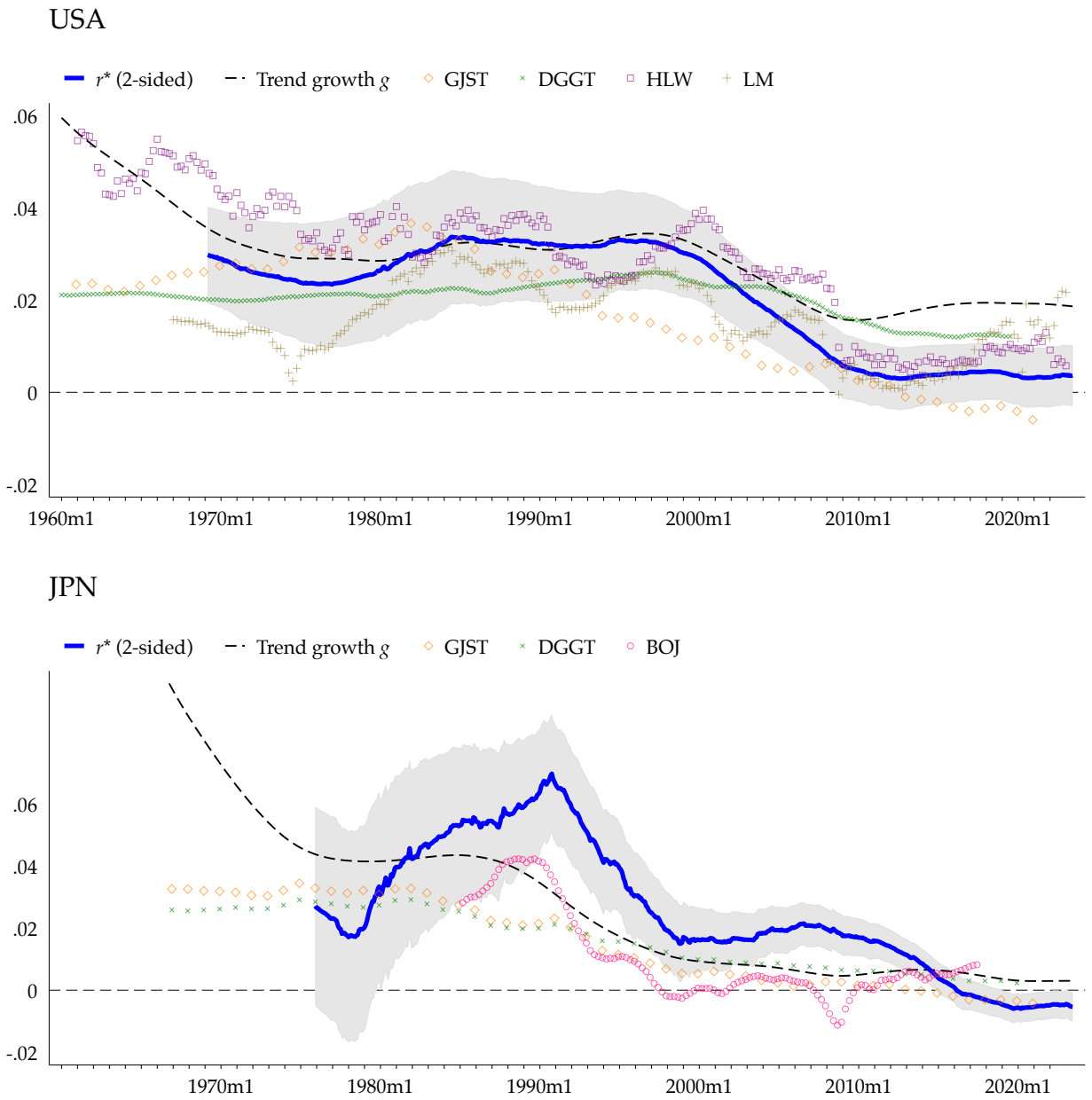

**Figure 6:** *Trends in r*, our estimates versus other estimates (continued)*

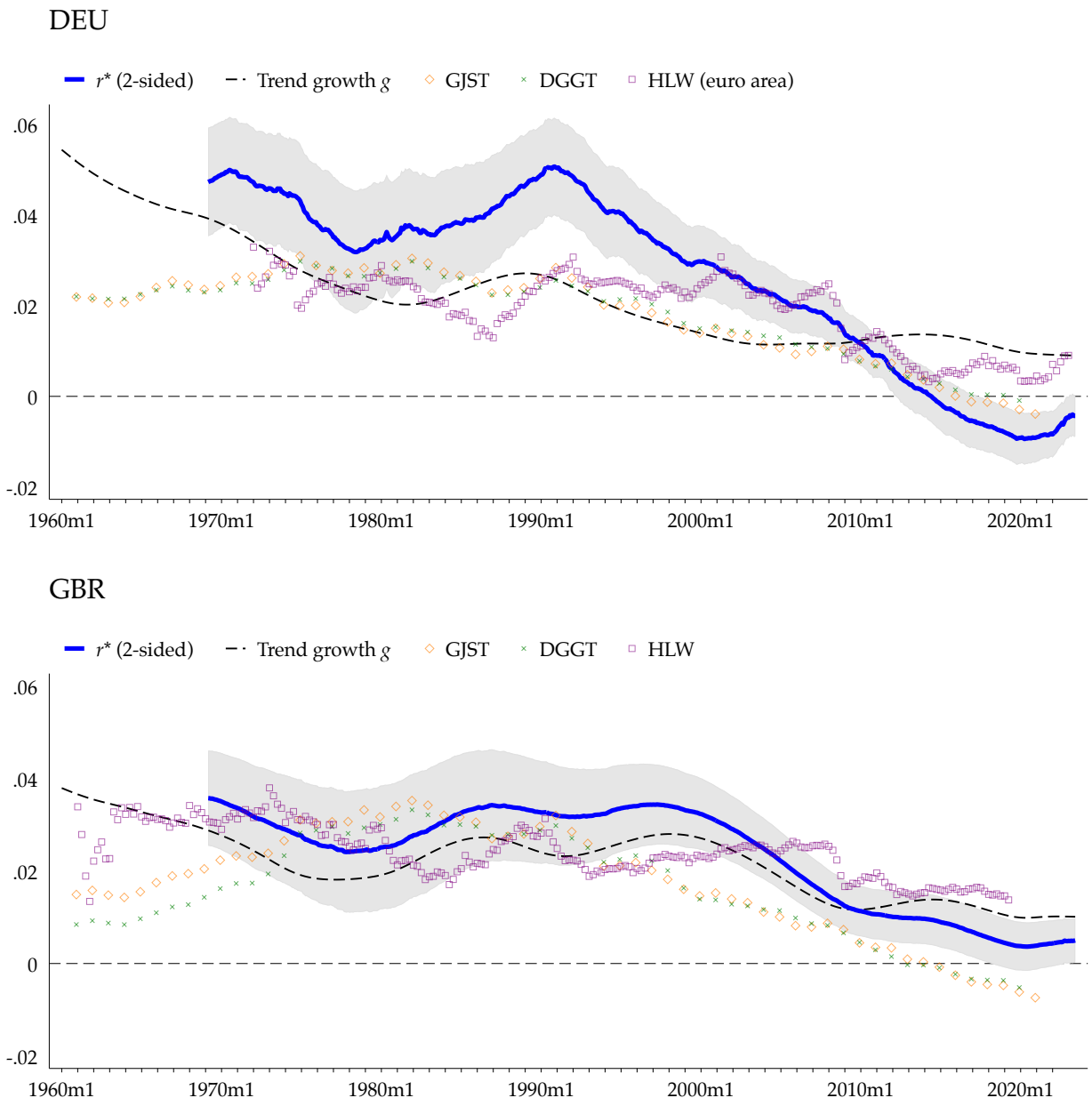

**Figure 6:** *Trends in r*, our estimates versus other estimates (continued)*

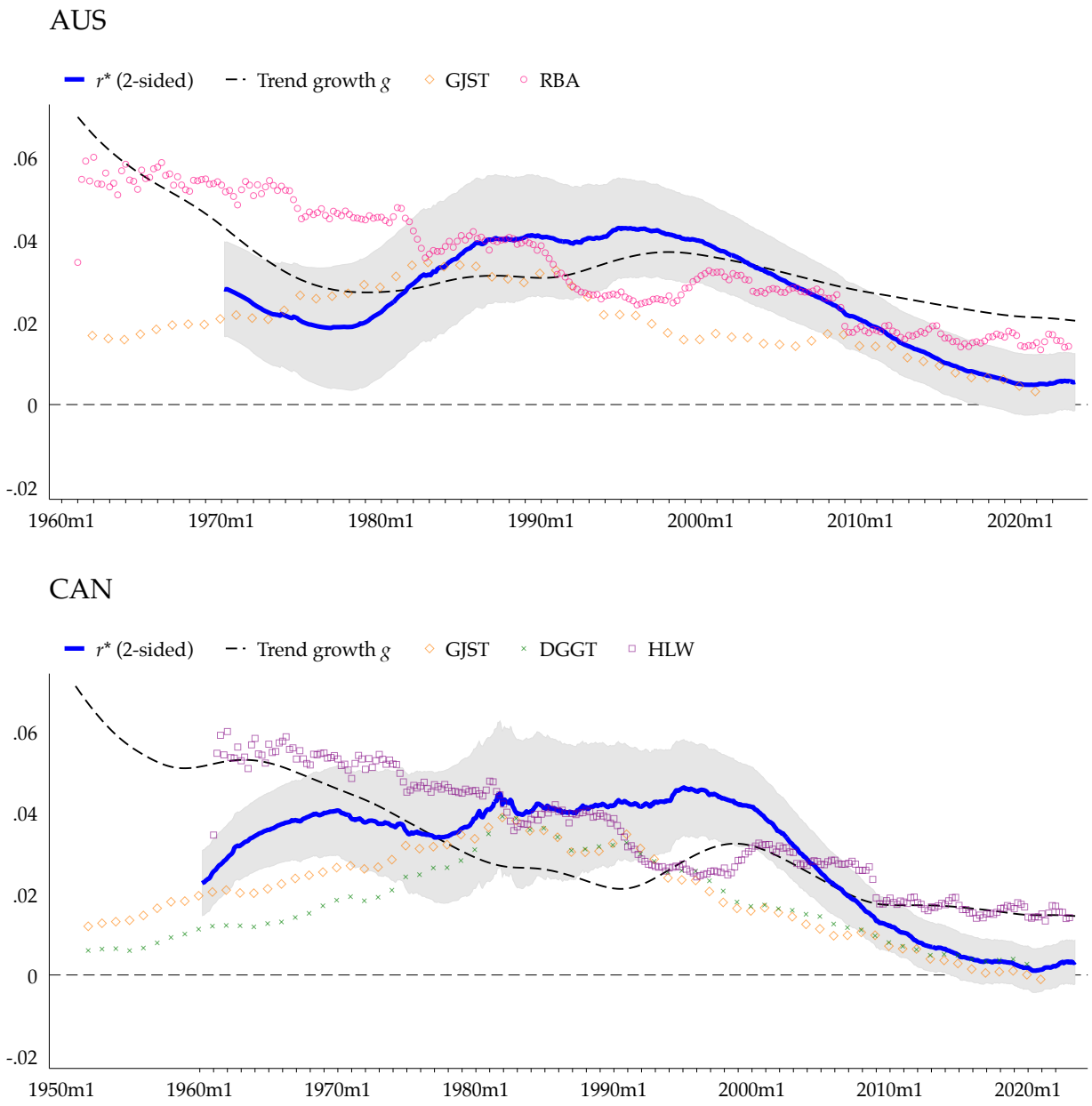

**Figure 6:** *Trends in r*, our estimates versus other estimates (continued)*

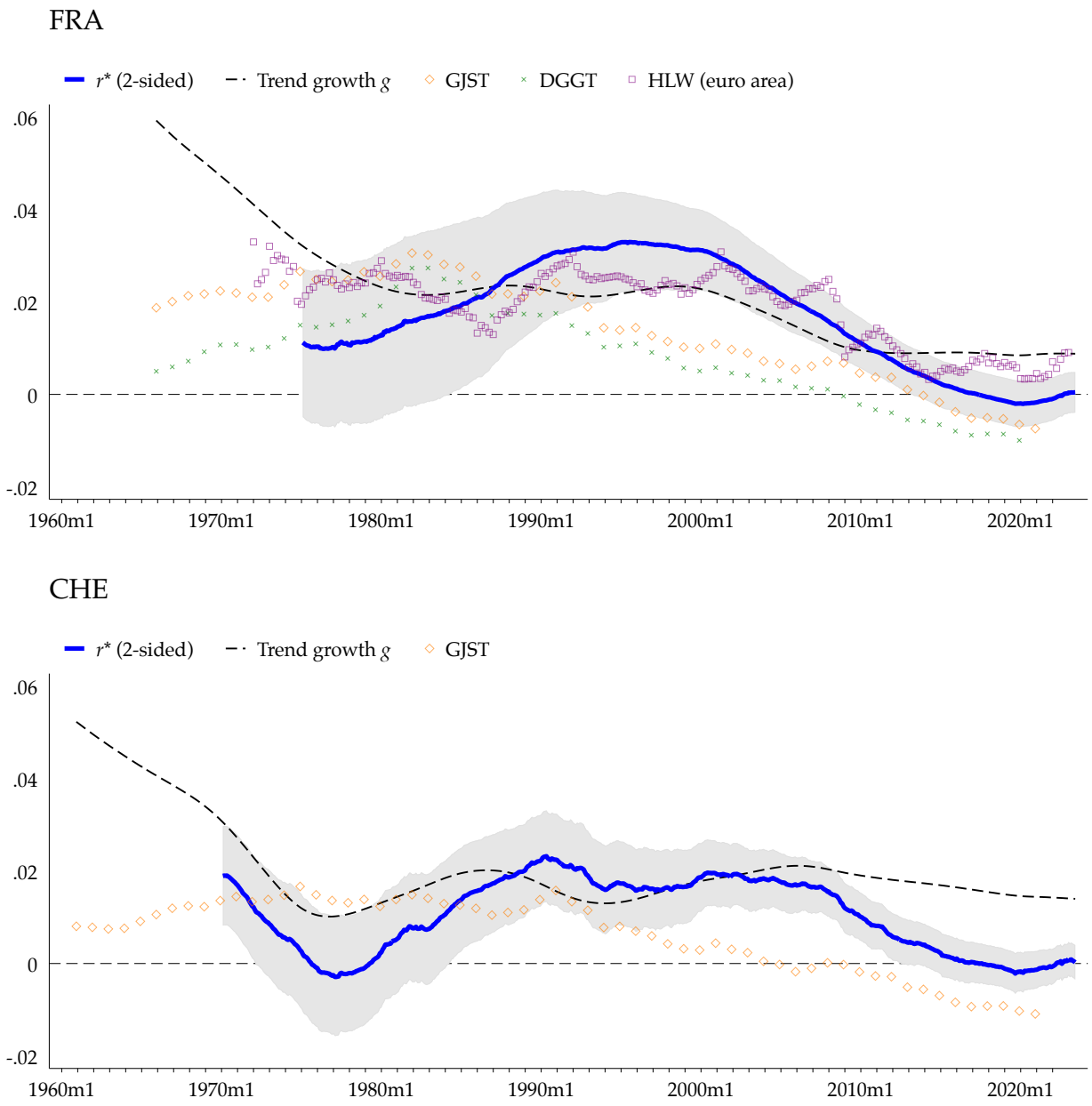

**Figure 6:** *Trends in r*, our estimates versus other estimates (continued)*

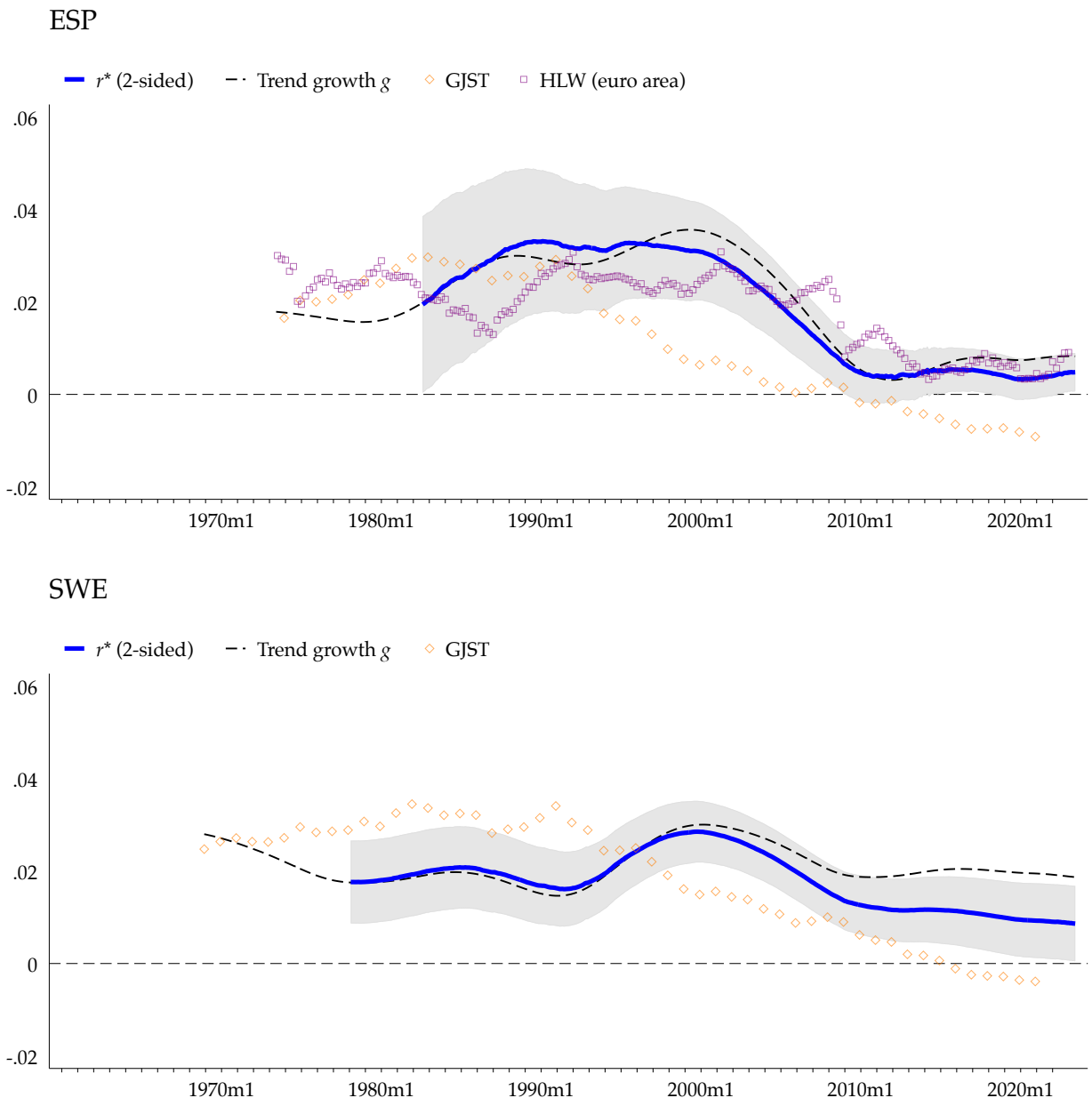

## 7.2. International comovements

The top panel in Figure 7 shows the $r^*$ estimates. Natural rates have fallen over time in all countries, but not monotonically, consistent with previous works documenting the decline of real rates over the long run (Jordà, Knoll, Kuvshinov, Schularick, and Taylor, 2019; Rogoff, Rossi, and Schmelzing, 2022). As recently as the 1990s, natural rates in these countries were between 100 and 600 bps. By the end of the sample 4 out of 10 countries have a negative $r^*$, and most others are between 0 and 50 bps. There is cross-country correlation, and natural rates have a positive correlation with the "global" component, and a considerable local component at high frequency. These comovements may reflect forces of market integration to some degree, as well as the effects of common factors.

We do see a general shift upwards across all countries in the 1970s–1980s, even if the timing varies from one country to the next. A strong coherence across countries is also seen in the sharp downward trend in $r^*$ that is set in motion around 1990. This was previously noted for one or two countries, starting with the U.S., and various explanations have been offered for that phenomenon, including not just slower growth but also demographics, the EM savings glut, the falling price of investment, among others (Rachel and Smith, 2017; Del Negro, Giannone, Giannoni, and Tambalotti, 2017; Rachel and Summers, 2019; Cesa-Bianchi, Harrison, and Sajedi, 2022). What we see here is how broadly that phenomenon was experienced across a wide swath of advanced economies.

Lastly, we see that the dispersion of natural rates falls over time At the start of each country's sample period, in the 1970s and 1980s, the natural rate estimates range widely with a max-min difference of around 400–500 bps.. But by the end of the sample in all 10 countries have a natural rate sit in a narrower interval between –100 and 100 bps. This would be consistent, mechanically, with convergence in either the $g$ or $z$ terms — which we discuss in a moment — and also aligns with the idea that under common forces (of demography or via globalization in technology or finance), in the long run, countries may be under the sway of a common global factor in $r^*$ (Clarida, 2019).

The top panel in Figure 8 shows the evolution of growth rates $g$. We can see two immediate implications from this chart. First, in line with common wisdom, trend growth rates have been declining inexorably during the postwar decades, with rare reversals. They have also tended to converge, but started to do so earlier than any convergence in natural rates. Thus, whilst some of the variation in the country-level natural rates $r^*$ across space and time can be explained by $g$, this is by no means the entire story and so much work is left for the residual.

The final panel in Figure 8 shows the important role played by the headwinds term $z$ in natural rates. We see the rise in this $z$ term, often more than offsetting the decline in growth, in the 1970–90 period, which is why natural rates tended to rise then. In contrast, the $z$ term reaches a peak around 1990, and then enters a secular decline in all countries. This relates to the global bond market "conundrum" — Greenspan's term — whereby the fall in real rates took on a pronounced turn beyond fundamentals alone. Seen here, the extra headwinds in the form of a fall in $z$ were experienced not just in the U.S. but across all advanced economies, consistent with trends, like demographics and investment prices, that were witnessed around the globe.

**Figure 7:** *Macro trends in $r^*$ and $\pi*$ in international data*

The top chart displays estimates of the natural rate $r^*$ and the bottom chart the measure of trend inflation $\pi^*$. The global component is the cross-country average in each period.

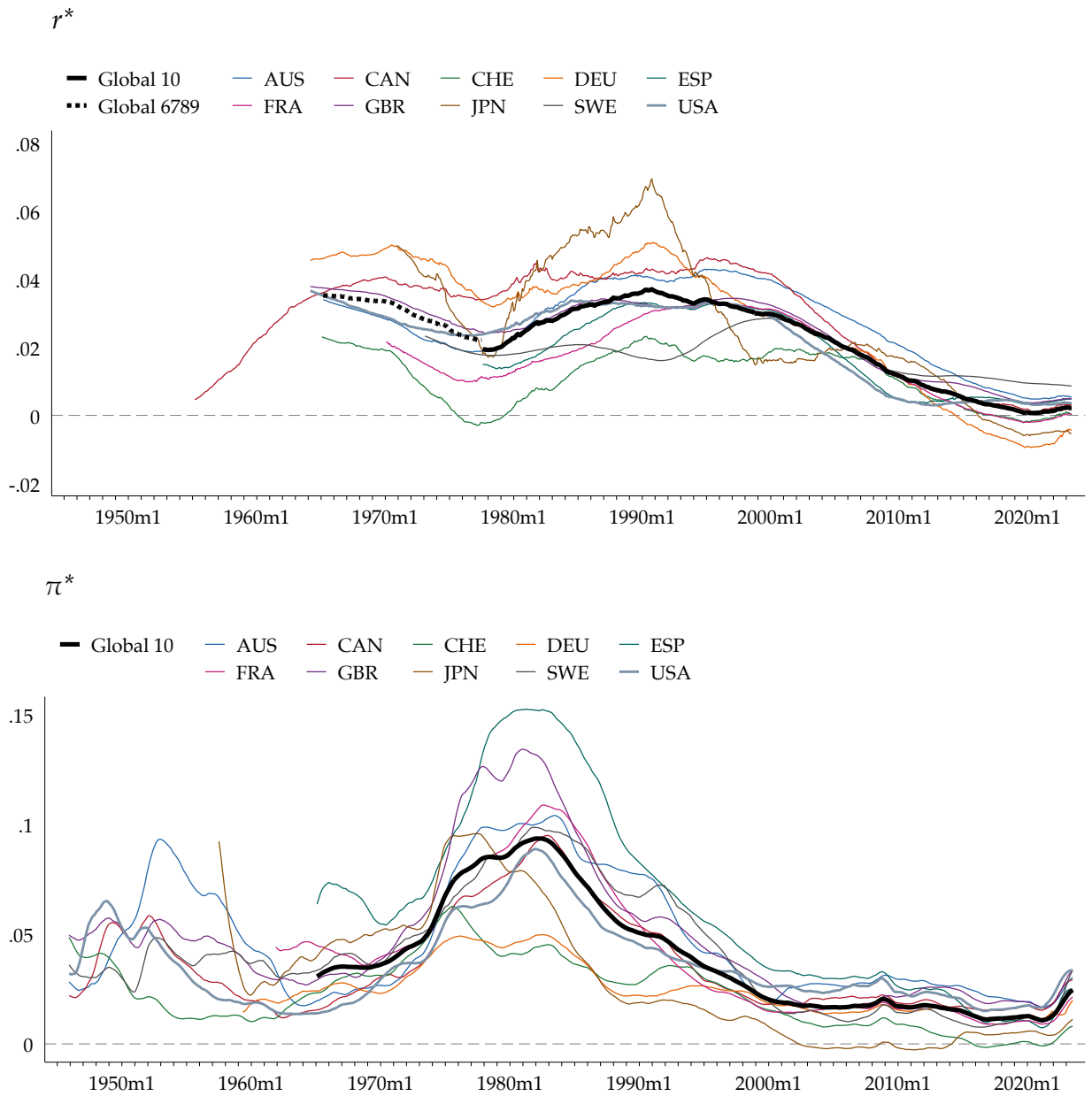

**Figure 8:** *Macro trends in g and z in international data*

The top chart displays the measure of trend growth $g$ and the bottom chart estimates of the headwind trend $z$. The global component is the cross-country average in each period.

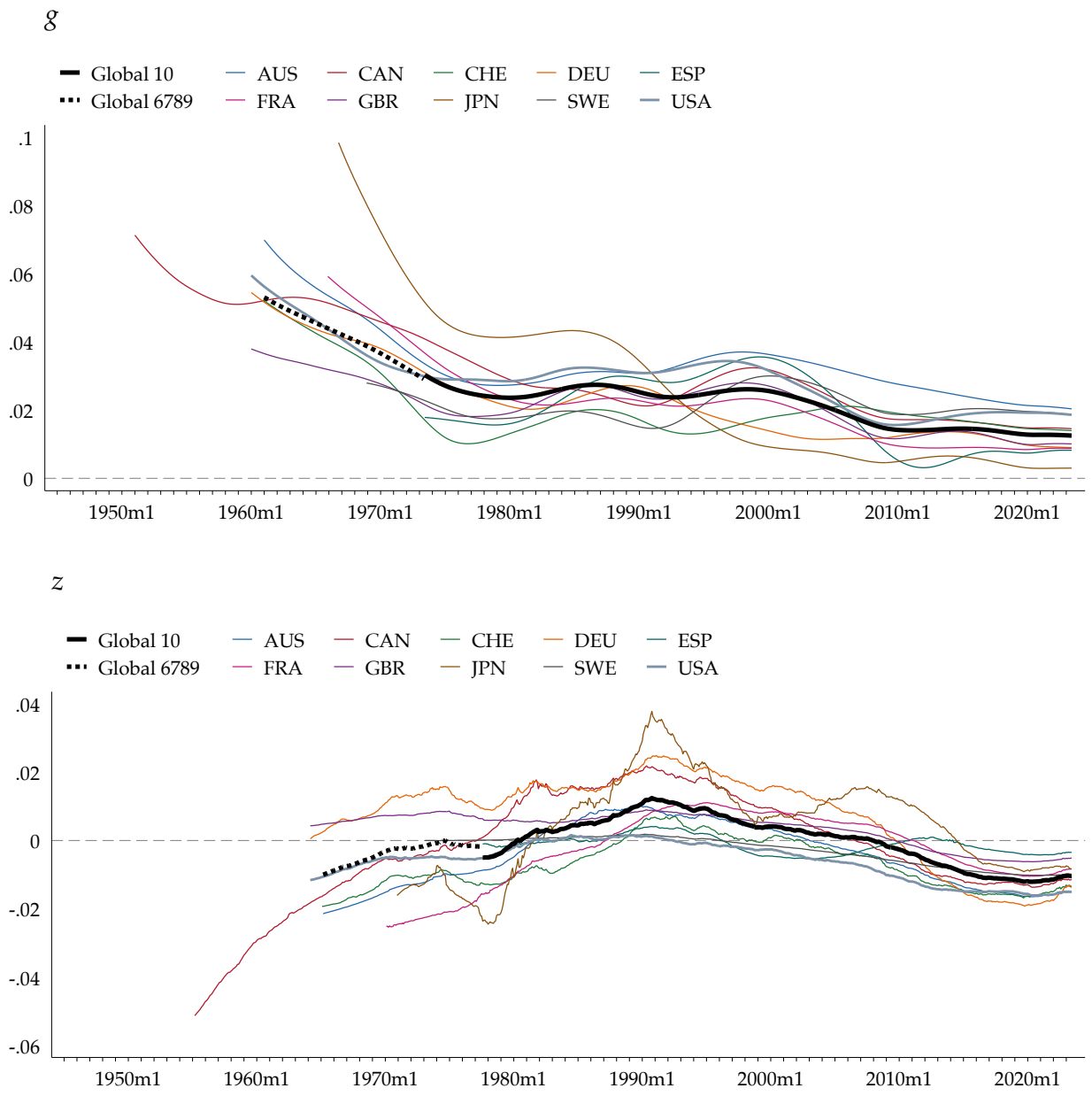

## 8. Major drivers of natural rates: growth and demography

In a final exercise we explore whether our new natural rate estimates are consistent with some of the prevailing explanations in the literature for the secular decline of natural rates over recent decades.

The two drivers we focus on are the rate of growth and demography, since these have been found to be consistent and dominant forces in many studies that have examined recent real rate trends (Carvalho, Ferrero, and Nechio, 2016; Rachel and Smith, 2017; Rachel and Summers, 2019; Eggertsson, Mehrotra, and Robbins, 2019; Cesa-Bianchi, Harrison, and Sajedi, 2022; Kopecky and Taylor, 2022) The literature has used a variety of calibrated equilibrium models (PE and GE) as well as reduced-form saving-investment models, to argue for the importance of these channels. But given the extent of our new natural rate estimates for 10 countries over many decades, we explore the question with a direct panel econometric approach.

**Panel estimating equation** We will suppose that the headwinds term $z$ depends on growth $g$, demography summarized by the age structure $\boldsymbol{D}$, and other factors $\boldsymbol{X}$, so that we can write $r^* = g + z = f(g, \boldsymbol{D}; \boldsymbol{X})$.

We will then assume that growth affects $r^*$ linearly as $\phi g$ , but not necessarily with a unit coefficient, since theory is ambivalent on this point. In a standard neoclassical model, as noted, the coefficient $c = 1/\sigma$ depends on the EIS parameter. But in life-cycle OLG models, growth can affect aggregate saving, since, all else equal, slower (higher) growth implies a need to save (borrow) more for smoothing. Conversely, buffer-stock motives may work in the opposite direction. On the investment side, lower growth typically entails less investment demand. Overall, then, higher growth $g$ may be associated with higher natural rates, with $\phi > 0$ as saving supply falls and investment demand rises.

Turning to the demography channel, a life-cycle OLG model with variable income and labor participation across age groups will also generate aggregate saving that depends on the population age shares, with young-adults saving little, or borrowing, middle-age adults saving a lot, and the older workers and retirees holding on to much of their wealth as a precaution to provide retirement income in a world of stochastic mortality and, possibly, also bequest motives. On the investment side, we also expect more workers (non-workers) to be associated with higher (lower) investment demand.[8]

In sum, these modeling assumptions align with the standard intuition that, all else equal, the age structure of the population $\boldsymbol{D}$ will have an inverted-U shaped relationship with $r^*$, with net positive effects from younger-age lower-wealth people in work, and net negative effect from older higher-wealth people near to or in retirement. As we see below, this intuition will turn out to be consistent with the empirical evidence.

[8]Various works have examined demographic impacts on consumption, saving and investment quantities. See, e.g., Aksoy, Basso, Smith, and Grasl (2019) and Kopecky (2023).

We want to estimate the empirical relationship between growth, population structure, and $r^*$. A saturated approach would be to estimate a panel country fixed-effects model

$$r^*_{it} = a_i + \phi g_{it} + \sum_{j=1}^{J} \alpha_j p_{j,it} + \theta \boldsymbol{X}_{it} + \epsilon_{it}\,, \tag{27}$$

where $p_{j,it}$ is the population age share in bin $j$, in country $i$, at time $t$, and wlog the $\alpha_j$ sum to one.

For parsimony, and to avoid overfitting to a large number of age shares, we follow Kopecky and Taylor (2022) and fit a Fair and Dominguez (1991) cubic polynomial function to a finite set of age bins $j = 1, \ldots, J$, with $J = 12$, with $\alpha_j$ are fit with a polynomial $\alpha_j = \gamma_0 + \gamma_1 j + \gamma_2 j^2 + \gamma_3 j^3$, with $\gamma_0$ obtained from the restriction that the $\alpha_j$ sum to one.

We then define

$$D_{1,it} = \left( \sum_{j=1}^{J} j\, p_{j,it} - \frac{1}{J} \sum_{j=1}^{J} j \right)\,,\; D_{2,it} = \left( \sum_{j=1}^{J} j^2\, p_{j,it} - \frac{1}{J} \sum_{j=1}^{J} j^2 \right)\,,\; D_{3,it} = \left( \sum_{j=1}^{J} j^3\, p_{j,it} - \frac{1}{J} \sum_{j=1}^{J} j^3 \right)\,. \tag{28}$$

An equivalent linear estimating equation, absorbing all other factors $\boldsymbol{X}$ into the error term, is then

$$r^*_{it} = a_i + \phi g_{it} + \sum_{k=1}^{3} \gamma_k D_{k,it} + \epsilon_{it}\,, \tag{29}$$

and estimates of the $\alpha_j$ terms can be recovered from the estimated $\gamma_k$.

**Model estimates, drivers and predictions** To estimate this equation we take our annual natural rate estimates $r^*_{it}$ for all 10 countries, along with growth rates $g_{it}$, over the post-1970 sample and merge them with annual UN population age-structure estimates, as used in Kopecky and Taylor (2022), from which the $D_{1,it}, D_{2,it}, D_{3,it}$ terms can be built. This yields an almost-balanced panel of about 500 observations. The resulting estimates are shown in Table 5 and the implied $\alpha_j$ effects by age bin are shown in Figure 9.

The baseline model in Column (1) fits will with an $R^2$ of 0.60. A model with quartic and quintic polynomial terms was found to fit no better, as those higher-order terms were not statistically significant, so we stick to the cubic approximation. The cubic term is small and positive, and so in the relevant range the approximation is close to quadratic, but flatter to the right as $j$ increases. The coefficient on growth is positive, as expected, but the effect is less than one-for-one. The age effects follow the expected inverted-U shape, with young adults ages 20–49 having a net positive effect on $r^*$, but older adults 55+ having a net negative effect. To guard against spurious regression with trending variables in Column (2) we also estimated the model with a time trend (year minus 2000) but the results were very similar, with a mild global time trend of minus 3.74 bps per year.

We now want to ask how well this empirical model can fit the observed historical data. The evolution of the right-hand-side variables since 1970 can tell us right away that the model has the

**Table 5:** *Empirical model of natural rates using Fair and Dominguez (1991) age effects specification*

This table shows estimates of the Fair and Dominguez (1991) model using cross-country panel data. See text.

| | (1) $r^*$ | (2) $r^*$ |
|---|---|---|
| $g$ | $0.498^{***}$ | $0.478^{***}$ |
| | (0.056) | (0.054) |
| $D_1$ | $0.222^{***}$ | $0.221^{***}$ |
| | (0.023) | (0.022) |
| $D_2$ | $-0.0348^{***}$ | $-0.0302^{***}$ |
| | (0.0047) | (0.0046) |
| $D_3$ | $0.00143^{***}$ | $0.00112^{***}$ |
| | (0.00025) | (0.000250) |
| Time trend | | $-0.000365^{***}$ |
| | | (0.000059) |
| Constant | $0.0289^{***}$ | $0.0374^{***}$ |
| | (0.0028) | (0.0030) |
| $N$ | 543 | 543 |
| $R^2$ | 0.604 | 0.631 |

Note: Standard errors in parentheses. $^{*}$ $p < 0.05$, $^{**}$ $p < 0.01$, $^{***}$ $p < 0.001$.

**Figure 9:** *Implied $\alpha_j$ effects of population share on r* by age bin*

This figure shows implied age effects based on the Fair and Dominguez (1991) model estimates. See text.

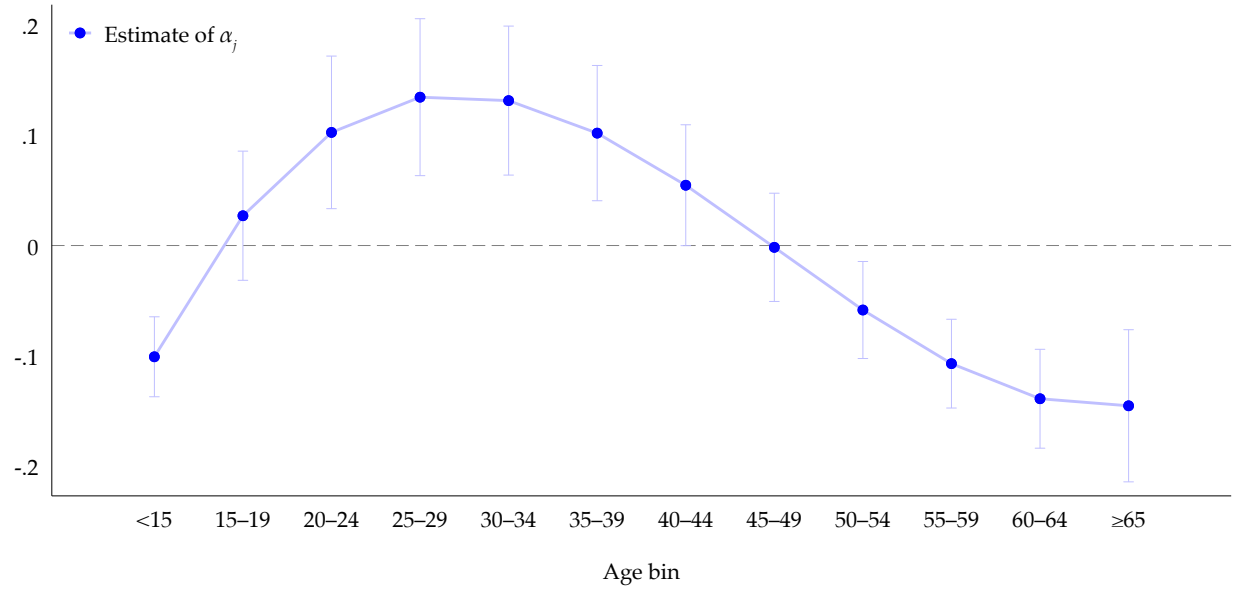

**Figure 10:** *Trends in the over-55 age share in each country after 1970*

This figure shows annual UN population age-structure estimates as used in Kopecky and Taylor (2022). The global component is the cross-country average in each period.

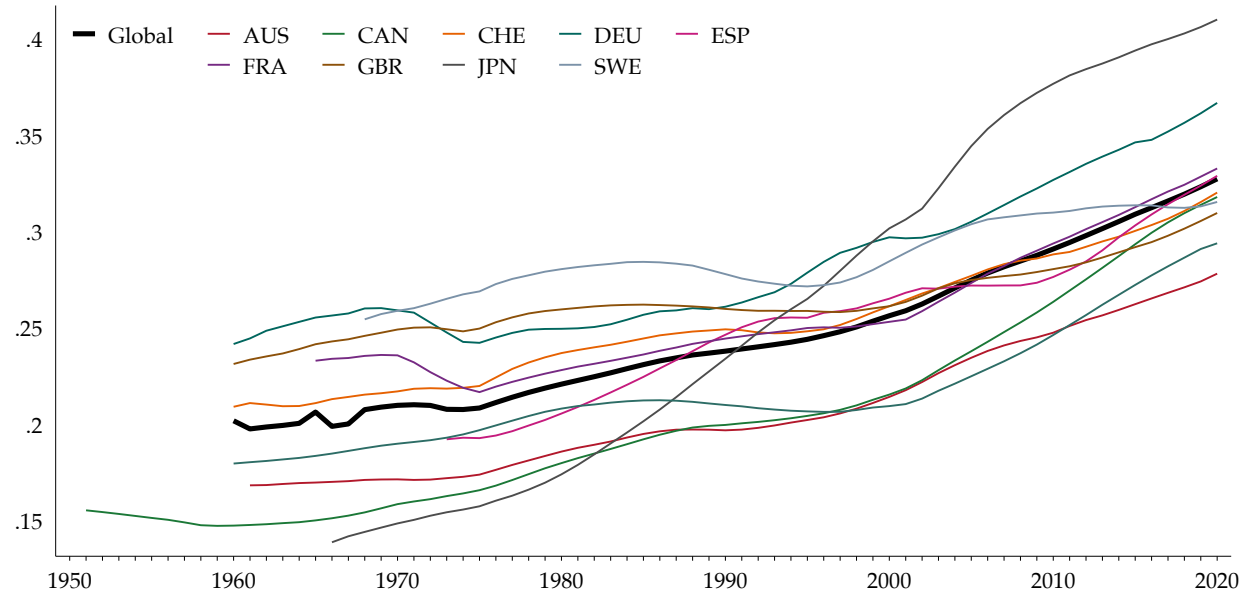


potential to work, as is well known. Looking at these underlying drivers in growth (Figure 8) and aging (Figure 10), the patterns are clear and consistent. Over 50 years, the rate of growth in the advanced economies steadily declined, with some cross-sectional timing variation. And, over those same 50 years, the over 55 age-share in the advanced economies steadily rose, again with some timing variation. In both cases, the trends become stronger and more uniform across countries from the 1990s onwards. And in both cases, the trends were most extreme in Japan, as is also well known.

To evaluate the fit, we take the model and compare the actual and fitted values of $r^*_{it}$. For clarity, we demean by country, and aggregate observations into quinquennial averages. The results are shown as a scatter plot in Figure 11. Here countries move from top right towards bottom left, over time, although some reversals happen along the way as growth and demographic factors fluctuate.

What might be surprising is that the model fit is quite respectable. The correlation of actual and fitted natural rates is about $^2/_3$, as is the slope of the line of best fit for these data ($\beta = 0.61$, as shown). In Japan both the actual and fitted natural rate fell by about 600 bps. The fit is good, and close to the 45-degree line, for the case of Japan, suggesting a close to 100% explanatory power. In other countries the decline is 300 bps or less, and shallower slope explains the resulting overall fit.

Thus, in our new and large sample of $r^*$ estimates for 10 advanced economies, examining covariates across time and space we find a strong role for growth and demography as potential drivers of declining real rates, which serves to corroborate and extend previous theoretical decompositions based on "global" natural rate estimates built for a single group aggregate of advanced economies

**Figure 11:** *Actual and fitted natural rates from the empirical model after 1970*

This scatter plot shows the actual and fitted values of the natural rate from the empirical Fair and Dominguez (1991) model using cross-country panel data on growth rates and demographic structure. The line of best fit is also shown and its slope. See text.

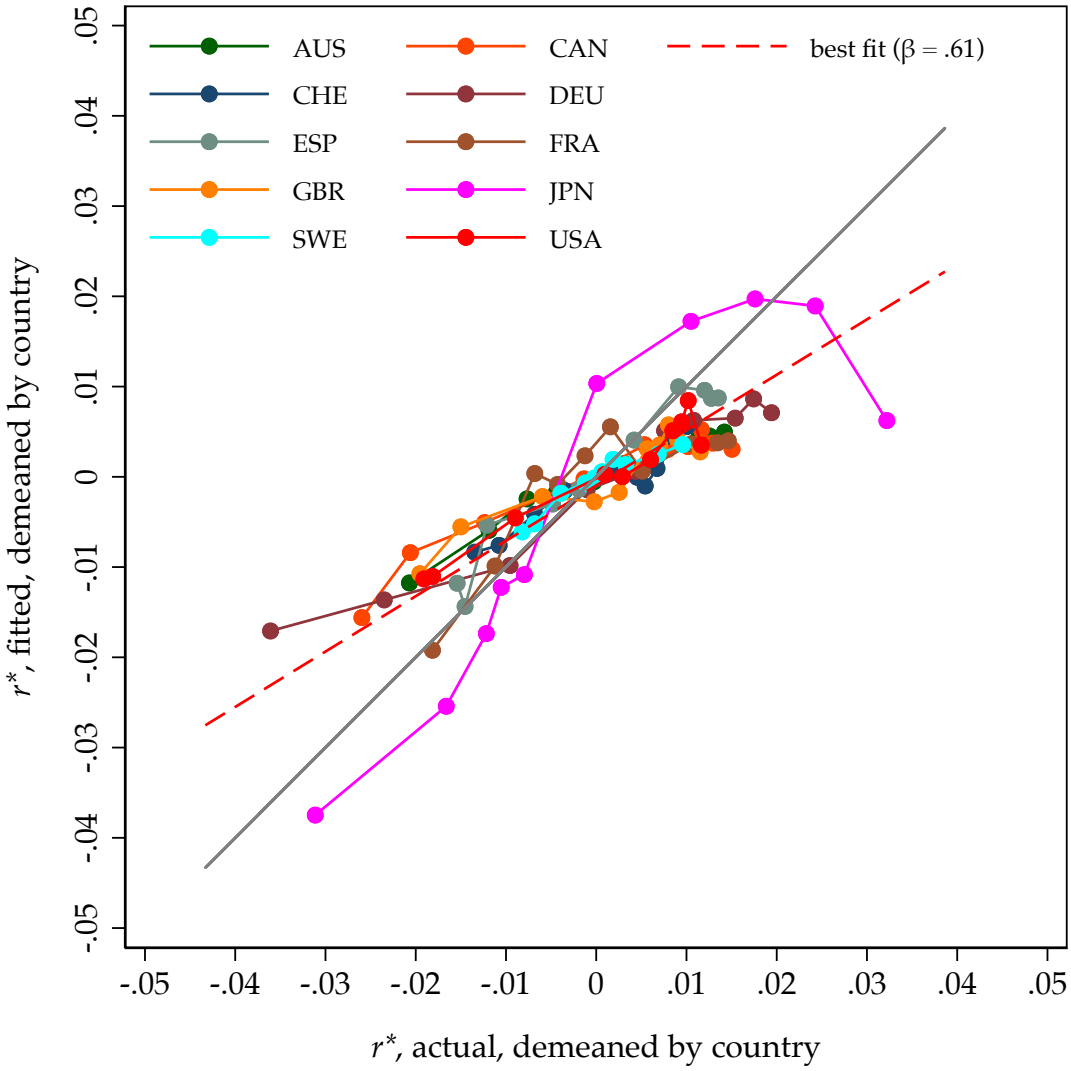

(cf. Rachel and Summers, 2019; Cesa-Bianchi, Harrison, and Sajedi, 2022).

## 9. Conclusion: The evolving global bond market

The finance approach to interest rates uses term-structure models of the yield curve but excludes macro factors. The macro approach to interest rates in the Wicksellian tradition links to growth but downplays financial market information. We propose a bridge between these approaches and utilize both macro and financial market information in the simplest encompassing model where slow-moving macro trends in inflation and the natural rate serve as important factors for bond pricing, in additional to a single high-frequency cylical factor.

Our Kalman filter estimates of the latent natural rate have trends and turning points much like consensus macro estimates, and they tend to converge over time to a common path, but they differ in being typically somewhat lower on average in the recent years than most of the other estimates. We find bigger "headwinds" with natural rates converging near zero or even negative in all 10 countries by 2020, intensifying concerns about secular stagnation and proximity to the effective lower-bound on monetary policy in advanced economies. Mapping our estimates of the natural rate into growth and demographic drivers, we find that these two contributing factors can explain most of the decline seen since the 1970s. If economic and population forecasts of continued slow growth and further aging in advanced economies materialize, and absent other major shocks or jumps, then natural rates will remain in the vicinity of zero to 100 bps (with about $\pm 75$ bps confidence intervals). Interestingly, as of the end of our sample in June 2023, the country trends in natural rates have typically not reverted upwards dramatically in the current policy rate cycle.

Returning to the puzzle identified in section 2 via the limiting forward decomposition equation Equation 1, we turn to Figure 12 where we reconsider long run trends post-1980 in light of our new natural rate estimates. Recalling the notation $f - \pi - r^* = RP$, we plot forward rates (10y-10y), then we subtract inflation and our new natural rate estimate to infer the proxy limiting bond risk premium term, showing all these time series for all 10 countries. We then plot the series for the expected excess return generated by our model above and also the bond risk premium derived from an ACM-style model. If one accepts our model, or the approximation from the limiting forward decomposition, then the flat path of the bond risk premium using those two estimation methods is similar, and quite different to the declining paths found using an ACM-style model.

Our results could point towards an alternative historical narrative of the bond market over 50+ years, a rather different story where risk premia are non-trending and follow paths that happen to be consistent with the type of model we presented where the assumptions lead to risk premia being driven by the cyclical, detrended price of risk factor alone. Take the U.S., where yields are often seen as driven by falling inflation and bond risk premia since the peak of inflation circa 1980. But as we noted, that interpretation rested on finance models of risk premia that exclude macro factors, and the same issues arise in other countries' traditional histories. Yet here, when we bring macro factors into consideration, we obtain a picture of mostly flat risk premia around the world in this

era, as seen in the figure, and hence instead a more dominant role for the downward macro trends in explaining the history of the global bond markets.

**Figure 12:** *Our estimates with the forward decomposition*

In this figure, the light blue short dash line shows the bond risk premium estimated using the limiting forward decomposition; the red dash line shows the bond risk premium (10-year term premium) estimated using an ACM-style model fitted to each country; the solid blue line shows the expected excess return prediction from our model. Our model typically shows a flat bond risk premium trend similar to the forward decomposition, in contrast to the declining bond risk premium in the ACM-style model.

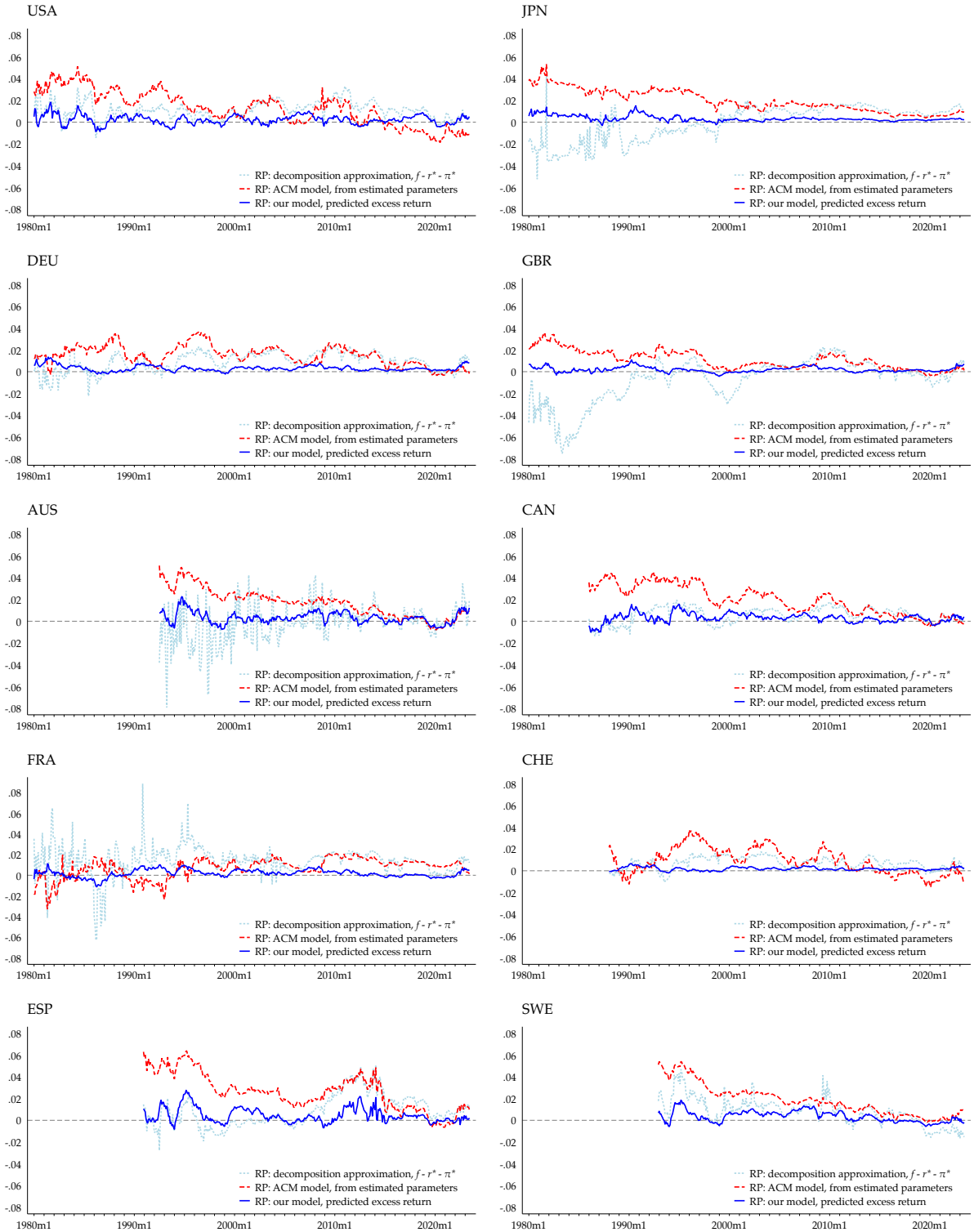

# References


Adrian, Tobias, Richard K. Crump, and Emanuel Moench. 2013. Pricing the term structure with linear regressions. *Journal of Financial Economics* 110(1): 110–138.

Adrian, Tobias, Richard K. Crump, and Emanuel Moench. 2015. Regression-based estimation of dynamic asset pricing models. *Journal of Financial Economics* 118(2): 211–244.

Aksoy, Yunus, Henrique S. Basso, Ron P. Smith, and Tobias Grasl. 2019. Demographic structure and macroeconomic trends. *American Economic Journal: Macroeconomics* 11(1): 193–222.

Ang, Andrew, and Monika Piazzesi. 2003. A no-arbitrage vector autoregression of term structure dynamics with macroeconomic and latent variables. *Journal of Monetary Economics* 50(4): 745–787.

Bauer, Michael D., and Glenn D. Rudebusch. 2020. Interest Rates under Falling Stars. *American Economic Review* 110(5): 1316–54.

Cadorel, Jean-Laurent. 2022. The French Historical Yield Curve Since 1870. Paris School of Economics. Unpublished.

Campbell, John Y., and Robert J. Shiller. 1987. Cointegration and Tests of Present Value Models. *Journal of Political Economy* 95(5): 1062–1088.

Carvalho, Carlos, Andrea Ferrero, and Fernanda Nechio. 2016. Demographics and real interest rates: Inspecting the mechanism. *European Economic Review* 88: 208–226. SI: The Post-Crisis Slump.

Cesa-Bianchi, Ambrogio, Richard Harrison, and Rana Sajedi. 2022. Decomposing the drivers of Global R*. Bank of England Working Paper 990.

Cieslak, Anna, and Pavol Povala. 2015. Expected returns in Treasury bonds. *Review of Financial Studies* 28(10): 2859–2901.

Clarida, Richard H. 2019. The Global Factor in Neutral Policy Rates: Some Implications for Exchange Rates, Monetary Policy, and Policy Coordination. International Finance Discussion Papers 1244, Board of Governors of the Federal Reserve System.

Cochrane, John H., and Monika Piazzesi. 2005. Bond risk premia. *American Economic Review* 95(1): 138–160.

Del Negro, Marco, Domenico Giannone, Marc P. Giannoni, and Andrea Tambalotti. 2017. Safety, Liquidity, and the Natural Rate of Interest. *Brookings Papers on Economic Activity* 48(1): 235–316.

Del Negro, Marco, Domenico Giannone, Marc P. Giannoni, and Andrea Tambalotti. 2019. Global trends in interest rates. *Journal of International Economics* 118(C): 248–262.

Duffee, Gregory. 2013. Forecasting Interest Rates. In *Handbook of Economic Forecasting*, edited by Graham Elliott, Allan Timmermann, volume 2, chapter 7, 385–426. Amsterdam: North-Holland.

Duffee, Gregory R. 2011. Information in (and not in) the Term Structure. *The Review of Financial Studies* 24(9): 2895–2934.

Eggertsson, Gauti B., Neil R. Mehrotra, and Jacob A. Robbins. 2019. A Model of Secular Stagnation: Theory and Quantitative Evaluation. *American Economic Journal: Macroeconomics* 11(1): 1–48.

Fair, Ray C., and Kathryn M. Dominguez. 1991. Effects of the Changing U.S. Age Distribution on Macroeconomic Equations. *American Economic Review* 81(5): 1276–1294.

Grimm, Maximilian, Òscar Jordà, Moritz Schularick, and Alan M Taylor. 2023. Loose Monetary Policy and Financial Instability. NBER Working Paper 30958.

Grishchenko, Olesya V., Franck Moraux, and Olga Pakulyak. 2020. Fuel up with OATmeals! The case of the French nominal yield curve. *Journal of Finance and Data Science* 6: 49–85.

Gürkaynak, Refet S., Brian Sack, and Jonathan H. Wright. 2007. The US Treasury yield curve: 1961 to the present. *Journal of Monetary Economics* 54(8): 2291–2304.

Holston, Kathryn, Thomas Laubach, and John C. Williams. 2017. Measuring the natural rate of interest: International trends and determinants. *Journal of International Economics* 108: S59–S75. 39th Annual NBER International Seminar on Macroeconomics.

Jordà, Òscar, Katharina Knoll, Dmitry Kuvshinov, Moritz Schularick, and Alan M Taylor. 2019. The Rate of Return on Everything, 1870–2015. *Quarterly Journal of Economics* 134(3): 1225–1298.

Jordà, Òscar, and Alan M. Taylor. 2019. Riders on the Storm. In *Challenges for Monetary Policy*, Proceedings of a symposium sponsored by the Federal Reserve Bank of Kansas City, Jackson Hole, Wyo., August 23–24, 2019, 17–59. Kansas City, Mo.: Federal Reserve Bank of Kansas City.

Joslin, Scott, Kenneth J. Singleton, and Haoxiang Zhu. 2011. A New Perspective on Gaussian Dynamic Term Structure Models. *Review of Financial Studies* 24(3): 926–970.

Kim, Don H., and Jonathan H. Wright. 2005. An arbitrage-free three-factor term structure model and the recent behavior of long-term yields and distant-horizon forward rates. Finance and Economics Discussion Series 2005-33, Board of Governors of the Federal Reserve System.

Kopecky, Joseph. 2023. Population age structure and secular stagnation: Evidence from long run data. *Journal of the Economics of Ageing* 24: 100442.

Kopecky, Joseph, and Alan M. Taylor. 2022. The Savings Glut of the Old: Population Aging, the Risk Premium, and the Murder-Suicide of the Rentier. NBER Working Paper 29944.

Kozicki, Sharon, and P. A. Tinsley. 2001. Shifting endpoints in the term structure of interest rates. *Journal of Monetary Economics* 47(3): 613–652.

Laubach, Thomas, and John C. Williams. 2003. Measuring the natural rate of interest. *Review of Economics and Statistics* 85(4): 1063–1070.

Litterman, Robert B., and José Scheinkman. 1991. Common Factors Affecting Bond Returns. *Journal of Fixed Income* 1(1): 54–61.

Lubik, Thomas A., and Christian Matthes. 2015. Time-Varying Parameter Vector Autoregressions: Specification, Estimation, and an Application. *Federal Reserve Bank of Richmond Economic Quarterly* 101(4): 323–352.

Ludvigson, Sydney C., and Serena Ng. 2009. Macro factors in bond risk premia. *Review of Financial Studies* 22(12): 5027–5067.

McCririck, Rachael, and Daniel Rees. 2017. The Neutral Interest Rate. *RBA Bulletin* (September): 9–18.

Nelson, Charles, and Andrew F. Siegel. 1987. Parsimonious Modeling of Yield Curves. *Journal of Business* 60(4): 473–89.

Okazaki, Yosuke, and Nao Sudo. 2018. Natural Rate of Interest in Japan: Measuring its size and identifying drivers based on a DSGE model. Working Paper Series 18-E-6, Bank of Japan.

Piazzesi, Monika. 2010. Affine Term Structure Models. In *Handbook of Financial Econometrics: Tools and Techniques*, edited by Aït-Sahalia, Yacine, and Lars Peter Hansen, volume 1 of *Handbooks in Finance*, chapter 12, 691–766. Amsterdam: North-Holland.

Rachel, Lukasz, and Thomas D. Smith. 2017. Are Low Real Interest Rates Here to Stay? *International Journal of Central Banking* 13(3): 1–42.

Rachel, Łukasz, and Lawrence H. Summers. 2019. On Secular Stagnation in the Industrialized World. *Brookings Papers on Economic Activity* (Spring): 1–54.

Rogoff, Kenneth S., Barbara Rossi, and Paul Schmelzing. 2022. Long-Run Trends in Long-Maturity Real Rates 1311–2021. NBER Working Paper 30475.

Svensson, Lars E. O. 1994. Estimating and Interpreting Forward Interest Rates: Sweden 1992–1994. NBER Working Paper 4871.

Wright, Jonathan H. 2011. Term Premia and Inflation Uncertainty: Empirical Evidence from an International Panel Dataset. *American Economic Review* 101(4): 1514–34.

# A. Appendix

## Bayesian estimation of the state-space model

We estimate the model using Bayesian inference. First, Bayesian methods are a potent framework to handle latent variables in state-space models as the one presented here. Second, it allows us to use prior distributions to regularize the estimation of the unobserved low-frequency macroeconomic and high-frequency financial drivers in the model. In particular, it allows us to impose priors that ensure that the headwinds factor, $z_{t+1}$, captures structural macroeconomic phenomena.

Bayesian inference constructs a posterior distribution $p(\theta|Y)$ by combining a likelihood $p(Y|\theta)$ and prior distribution $p(\theta)$ as follows

$$p(\theta|Y) = \frac{p(Y|\theta)p(\theta)}{p(Y)} \tag{30}$$

where $Y$ is the set of observations, and the marginal data density $p(Y)$ is a normalization constant independent of the estimated parameters $\theta$. Since we cannot easily compute moments of the posterior $p(\theta|Y)$ or directly sample from it, we use a random-walk Metropolis-Hastings (RWMH) algorithm, a Markov chain Monte Carlo (MCMC) method, to sample from the posterior $p(\theta|Y)$.

We then estimate the state-space model using the RWMH algorithm for each country separately. The algorithm builds a Markov chain of posterior draws $\{\theta_n\}_{n=0}^{N}$ which give rise to a sequence of posterior distributions $\{p_n(\theta|Y)\}_{n=0}^{N}$, with the last draw in the sequence being equal to the posterior distribution. At each step $n$, the algorithm propagates the parameter vector, or the particles $\theta_{n-1}$, such that over the whole sequence, the parameter vector $\{\theta_n\}_{n=0}^{N}$ represents the target distribution $p(\theta|Y)$. Thus, at each step $n$, the algorithm draws a new proposal particle $\vartheta_n$, conditional on the previous particle $\theta_{n-1}$, the set of observations $Y$, and the proposal density $q(\cdot|\cdot)$. We accept step $n$ draw $\vartheta_n$ with probability

$$\alpha\left(\vartheta_n|\theta_{n-1}\right) = \min\left\{\frac{p(Y|\vartheta_n)p(\vartheta_n)/q(\vartheta_n|\theta_{n-1})}{p(Y|\theta_{n-1})p(\theta_{n-1})/q(\theta_{n-1}|\vartheta_n)}\right\}, \tag{31}$$

where the step $n$ likelihood function $p(Y|\vartheta_n)$ is computed using the Kalman filter on the state-space representation of the model determined by equations Equation 24 and Equation 25. The RWMH algorithm sets the proposal distribution to

$$q\left(\cdot|\theta_{n-1}\right) = N\left(\theta_{n-1}|\mathfrak{c}\cdot\widehat{\Sigma}\right). \tag{32}$$

Formally, the algorithm proceeds as follows

1. **Initialization:** The initial particles are drawn from the prior distribution $\theta_0 \sim p(\theta)$.
2. **Recursive updates:** For $n = 1, ..., N$ recursively update the particle sequence
   (a) Draw step $n$ proposal particles $\vartheta_n$ from $q\left(\vartheta_n|\theta_{n-1}\right)$
   (b) Accept new draw with probability $\alpha\left(\vartheta_n|\theta_{n-1}\right)$
   (c) Update the particle sequence: If accepted $\theta_n = \vartheta_n$, else $\theta_n = \theta_{n-1}$
3. Remove the burn-in samples and construct posterior estimates as follows

$$\bar{h} = \frac{1}{N}\sum_{n=1}^{N} h(\theta_n)$$

$\widehat{\Sigma}$ is a diagonal matrix with entries from the prior variance of the model parameters. We set the constant $\mathfrak{c} = 0.4$ to target an acceptance rate of 23.4 percent, as it is the standard for the optimal acceptance target in Metropolis algorithms. Our estimation is calculated with a number of simulations equal to 50,000. Using the posterior mean of the obtained particle sequence as the estimator for the parameter vector $\theta$, we rerun the state-space model to construct our results. However, we also experimented with using the median and mode which did not affect the results.

For each country, we use as input information the inflation expectations measure $\pi_t^*$ and the real GDP series. We obtain the trend GDP series by applying the HP filter over quarterly GDP data with a smoothing parameter equal to $25,600 = 1600 \cdot 16$. The series thus obtained is interpolated to monthly data, and the trend growth rate $g_t$ is then calculated.

Our identification assumption is $r^*$ cointegrates with the trend GDP series, and that the difference has mean reversion properties compatible with a half-life within business cycle frequency, and not higher. This avoids the problem of $r^*$ acting as a residual term that would capture high-frequency oscillations in bond markets.

## Prior specification

We use the prior specification to impose parameter restrictions informed by existing estimates from the literature as well as by our view of the economic meaning of parameters. Most notably, we inform the priors of the headwinds and cyclical factors, ($z_t$ and $\epsilon^{cyc}$), to reflect the view that the headwinds factor captures structural macroeconomic phenomena with a frequency similar to that of macroeconomic series while the cyclical factor captures financial phenomena with a frequency similar to that of financial series. We specify relatively loose priors for the parameters in the model, as detailed in Table A.1, to allow for the estimation to add information. To further restrict the priors, we use a common prior structure across all countries. In particular, the prior specifications for all parameters other than the prior volatilities of the headwinds and cyclical factors, $\sigma_z$ and $\sigma_y$, are the same across countries. To account for the fact that the relative volatility of financial and macroeconomic data varies across countries, we tie the prior distributions for $\sigma_z$ and $\sigma_y$ to the observed yield and GDP data of each country in a systematic way, as detailed below.

- The persistence parameter $\rho_z$ is chosen to be close to unit root, but within the unitary circle to prevent an explosive solution. Its magnitude is taken to match a half life of around 60 months, similar to that of macroeconomic series. This keeps the headwinds factor within business-cycle frequency and not higher. In a freer setting, this term would act as a residual in the Kalman system and would tend to capture high-frequency variations that are hard to identify given the data.

- The prior distributions of the volatilities of the headwinds factor, $\sigma_z$, and the cyclical factor, $\sigma_y$, are Gaussian and set to match a relatively small range of variation for the frequency of both factors. For each country i, the mean of the prior yield volatility, $\mu_{\sigma_y}(i)$, is set such that the resulting prior variance of the cyclical AR(1) process equals the variance of the observed yield series, thus,

$$\mu_{\sigma_y}(i) = \sqrt{\sigma^2(\bar{y}(i)) \left(1 - \mu_{\rho_y}^2\right)}$$

  where $\sigma(\bar{y}_i)$ is the standard deviation of the observed yield data in country $i$, and $\mu_{\rho_y}$ is the prior mean for the persistence of the cyclical AR(1) process which is the same across countries, as outlined above.

Similarly, for each country i, the mean of the prior headwinds volatility, $\mu_{\sigma_z}(i)$, is set such that the resulting prior variance of the headwinds AR(1) process equals the variance of trend GDP of country i.

$$\mu_{\sigma_z}(i) = \sqrt{\sigma^2(\bar{g}(i))\left(1 - \mu_{\rho_z}^2\right)}$$

Thus, the prior means reflect the relative volatility of the macroeconomic and financial series in each country. We set the variances of both prior distributions relatively loose.

- For the model coefficients $b_{r^*}$, $a_y$, and $b_\pi$ we specify loose Gaussian priors with large variances and coefficients centered around values that calibrate the U.S. experience relatively well in a simple regression context. In particular, the priors of $b_{r^*}$ and $b_\pi$ are centered around 1 which reflects a fisherian view in which average yields move one-for-one with trend inflation and real rates.

**Table A.1:** *Prior specification for model parameters*

| Parameter | Distribution | Mean | Variance |
|---|---|---|---|
| $\rho_z$ | Beta | 0.997 | $1.5 \times 10^{-6}$ |
| $\rho_y$ | Normal | 0.9 | $1.0 \times 10^{-2}$ |
| $\sigma_z$ | Log-Normal | $\mu_{\sigma_z}$(i) | $3.0 \times \mu_{\sigma_z}$(i)$\times 10^{-2}$ |
| $\sigma_y$ | Log-Normal | $\mu_{\sigma_y}$(i) | $3.0 \times \mu_{\sigma_y}$(i)$\times 10^{-2}$ |
| $a_y$ | Normal | 0.0 | $1.0 \times 10^{-3}$ |
| $b_\pi$ | Normal | 1.0 | $1.0 \times 10^{-1}$ |
| $b_{r^*}$ | Normal | 1.0 | $1.0 \times 10^{-1}$ |

Note: Here $\sigma_z(i)$ is constructed as described above for each country $i$.